Journal of Applied Analysis and Computation
Volume 15, Number 3, June 2025, 1330–1373
Website:http://www.jaac-online.com
DOI:10.11948/20240226

NUMERICAL ANALYSIS OF A GRAD-DIV STABILIZATION METHOD FOR THE OLDROYD MODEL OF ORDER ONE

Bikram Bir[1,2,†] and Deepjyoti Goswami[3]

Abstract This paper analyzes an inf-sup stable Galerkin mixed finite element method with a grad-div stabilization for the equation of the motion of the fluid arising in the Oldroyd model of order one. The main idea of the grad-div stabilization method is to add a stabilization term to the Galerkin approximation, which is very effective at a high Reynolds number. Optimal error bounds for the velocity in $L^\infty(\mathbf{L}^2)$-norm and the pressure in $L^2(L^2)$-norm are derived in the semidiscrete case with time remaining continuous. Then, a fully discrete scheme is analyzed by employing the backward Euler method, and optimal error estimates are derived. All these estimates are obtained with constants independent of the inverse of viscosity and for both the cases when the solution is as smooth as we want (has to satisfy nonlocal compatibility conditions) and when the solution is just smooth (compatibility conditions are no longer needed). Finally, we present some numerical results in support of our theoretical findings.

Keywords Oldroyd model of order one, grad-div stabilization, backward Euler method, optimal error estimates.

MSC(2010) 65M60, 65M15, 35Q35.

1. Introduction

In this paper, we consider a linear viscoelastic model with a memory of past deformation. The model is known as the Oldroyd model of order one [36], and is given by the following integro-differential system:

$$\mathbf{u}_t - \mu\Delta\mathbf{u} + \mathbf{u}\cdot\nabla\mathbf{u} - \int_0^t \beta(t-\tau)\Delta\mathbf{u}(s)\,ds + \nabla p = \mathbf{f}, \quad \text{in } \Omega,\ t>0, \tag{1.1}$$

with incompressibility condition

$$\nabla\cdot\mathbf{u} = 0, \qquad \text{on } \Omega,\ t>0, \tag{1.2}$$

[†]The corresponding author.
[1]Department of Mathematics, Indian Institute of Technology Bombay, Mumbai, Maharashtra-400076, India
[2]Department of Mathematics, The Assam Royal Global University, Guwahati, Assam-781035, India
[3]Department of Mathematical Sciences, Tezpur University, Sonitpur, Assam-784028, India
Email: bikram@math.iitb.ac.in(B. Bir),
deepjyoti@tezu.ernet.in(D. Goswami)

and initial and boundary conditions

$$\mathbf{u}(x,0)=\mathbf{u}_0 \quad \text{in } \Omega, \quad \mathbf{u}=0, \quad \text{on } \partial\Omega, \ t\geq 0. \tag{1.3}$$

Here Ω is a bounded domain in $\mathbb{R}^2$ with boundary $\partial\Omega$, $\mu=\kappa\lambda^{-1}>0$, the kernel $\beta(t)=\gamma e^{-\delta t}$, $\gamma=\lambda^{-1}(\nu-\kappa\lambda^{-1})>0$ and $\delta=\lambda^{-1}>0$, where $\nu>0$ is the kinematic coefficient of viscosity, $\lambda>0$ is the relaxation time and $\kappa>0$ is the retardation time. The unknowns $\mathbf{u}$ and p represent the fluid's velocity and pressure, respectively. Furthermore, the forcing term $\mathbf{f}$ and the initial velocity $\mathbf{u}_0$ are given functions in their respective domains of definition. This system represents a basic model for polymeric fluids, suspensions, or biological fluids, a non-Newtonian model, which has been derived under the assumption that the material can be regarded as a single stationary macroscopic element with small stress and strain rates and finds applications in various industries, like, paints, DNA suspensions, biological fluids, and some chemical industries. When $\gamma=0$, the system reduces to the well-known Navier-Stokes flows and, as such, can be considered as an integral perturbation of the Navier-Stokes equations. For more details on the mathematical model and physical background, we refer to [36].

Details of early developments of the model and continuous and semi-discrete cases can be found in [21, 24, 40] and references therein. Moreover, for time discretization, we refer to [6, 22, 41, 47]. There are several other works on this model based on finite elements and related frameworks; for example, see [1,5,20,33,35,49, 50], and references therein.

Galerkin mixed finite element for the model has been analyzed on a few occasions [21,24] with optimal error estimates. However, it is well known that similar to the Navier-Stokes equation (NSEs), the coupling of the velocity and the pressure, through the divergence-free term, is in fact not desirable. There are methods, for decoupling by various means, like the penalty method, the artificial compressibility method, the pressure correction method, the projection method, etc., which attempt to overcome this difficulty by means of artificial conditions. Work in these directions for the Oldroyd model can be found in [7,33,45,46,51]. Unfortunately, these methods are less sufficient when the Reynolds number is high. This is due to the domination of the advection term on the viscous term, which typically arises for small values of viscosity. It is handled via methods based on stabilization techniques like streamline upwind/Petrov-Galerkin(SUPG) method, residual-free bubbles enrichment method, local projection stabilization, and interior-penalty methods, see [9, 11–13]. In particular, in the SUPG method, a grad-div stabilization is included, which allows for achieving stability and accuracy for small values of viscosity.

In this paper, we add a grad-div stabilization term to the problem (1.1)-(1.3) and we analyze its effect for high Reynolds number. The main idea is to add a stabilization term with respect to the continuity equation to the momentum equation. It was first proposed by Franca and Hughes [16] to improve the conservation of mass in the finite element method. However, the method comes with several other benefits. For example, the use of grad-div stabilization results in improved convergence of preconditioned iteration when the stabilization parameter is too small [37]. The well-posed continuous solution as well as the accuracy and convergence of the numerical approximation for small values of viscosity [39] and the local mass balance of the system in numerical experiments [15] are observed while using grad-div. Moreover, it has been observed that using grad-div stabilization in the simulation of turbulent flows is sufficient for performing a stable simulation, see [32, Figure 3] and [42, Figure 7].

These observations lead us to the present paper: to derive the error bounds that do not depend on inverse powers of viscosity (that is, μ, in our case) for the Galerkin mixed finite element method with grad-div stabilization applied to the Oldroyd model of order one. This is not the first time that similar results have been achieved. In fact, in [17,18], de Frutos *et al.* have obtained error bounds with constants independent of inverse powers of viscosity for the evolutionary Oseen equations and the Navier-Stokes equations, respectively. There are a few recent works in this direction for incompressible flow problems [23, 30, 43, 44, 48], but to the best of our knowledge, no work is available for the Oldroyd model of order one. In this paper, we extend the analysis of [18] to the Oldroyd model of order one. As in [18], we have carried out our analysis for the initial velocity $\mathbf{u}_0 \in \mathbf{H}_0^1 \cap \mathbf{H}^m$ ($m > 2$ and we call it, $\mathbf{H}^m$-smooth initial data), as well as for the initial velocity $\mathbf{u}_0 \in \mathbf{H}_0^1 \cap \mathbf{H}^2$ (we call it, $\mathbf{H}^2$-smooth initial data). However, our proofs are shorter and less technically involved than those from [18]. Our analysis relies solely on the standard L^2-projection, and the standard approximation properties along with the discrete incompressibility conditions. Also, same analysis goes through for both the cases, that is, $\mathbf{H}^m$-smooth and $\mathbf{H}^2$-smooth cases for the linear and quadratic approximation unlike [18], see Subsection 3.2.

We note that the assumption of $\mathbf{H}^m$-smooth data comes at the cost of non-local compatibility conditions of various orders, for the given data, at time $t = 0$. Without these conditions, which do not arise naturally, the solutions of the Oldroyd model of order one can not be assumed to have more than second-order derivatives bounded in $L^2(\Omega)$ at $t = 0$ (see [21]). The analysis for $\mathbf{H}^2$-smooth initial data takes into account this lack of regularity at $t = 0$.

We would also like to point out that the analysis in both these cases does not differ by much. However, the analysis suggests that less regularity of the initial velocity puts a restriction on the order of finite element approximation when keeping estimates independent of the inverse of μ. For example, with $\mathbf{H}^2$-smooth initial data, we may get a maximum second-order convergence rate in the case of velocity, even if we employ higher-order approximations, see Remark 3.4.

It is well known that the suitable choice of stabilization parameter for any stabilized scheme is important for accuracy in numerical simulations. In the case of grad-div stabilization, a suitable choice of grad-div parameter ρ is shown to be $\mathcal{O}(1)$ for the Navier-Stokes equations and for inf-sup stable finite element pairs, in [37,38]. In [34], it is shown that error can be minimized for $\rho \approx 10^{-1}$. However, larger values of ρ may be needed in special cases, see [19]. A detailed investigation of the choice of grad-div stabilization parameter for the steady Stokes problem has been discussed in [29]. They have observed that the choice of grad-div parameter depends on the used norm, the mesh size, the type of mesh, the viscosity, the finite element spaces, and the solution. A similar analysis and numerical simulations have been seen in [3] for the steady-state Oseen problem and Navier-Stokes equations.

In this paper, we briefly look into this aspect. Based on the error estimate from Theorem 3.1, we have observed that $\rho = \mathcal{O}(1)$ is a suitable choice for stable mixed finite element spaces. Moreover, for the MINI element, the choice of ρ can be in the range of h^2 to 1, see Remark 3.3. Furthermore, some numerical experiments are carried out to verify the theoretical order of convergence. The effect of the grad-div stabilization is then verified for a benchmark problem. We have also shown numerically that the grad-div parameter depends on the mesh size, the type of mesh, the viscosity, and the finite element spaces. Finally, we have obtained the values of grad-div parameter ρ that minimize the $\mathbf{L}^2$ and $\mathbf{H}^1$ errors for the velocity and L^2 error for the pressure for a known solution.

The main results of this article consist of the following:

(i) Stability analysis of the semidiscrete solution with constant does not depend on inverse power of μ.

(ii) Optimal error estimates for the velocity in $L^\infty(\mathbf{L}^2)$-norm and for the pressure in $L^2(L^2)$-norm, where the error bounds are independent of μ^{-1}, that is, these results are valid for high Reynolds number.

(iii) Fully discrete optimal error estimates, for the velocity and the pressure, by applying a first-order backward Euler method for temporal discretization. The order of convergence for the velocity in $L^\infty(\mathbf{L}^2)$ norm and the pressure in $L^2(L^2)$ norm is $\mathcal{O}(h^k + \Delta t)$ when the finite element velocity space and the pressure space are approximated by k-th and $(k-1)$-th degree piecewise polynomial, respectively ($k > 1$), where h and Δt are the space and time discretization parameter, respectively. These results are valid for high Reynolds number as well.

(iv) Numerical experiments with known solution to verify the order of convergence and simulations for a couple of benchmark problems to prove the effectiveness of the grad-div stabilization for the Oldroyd model of order one.

(v) Suitable choice of grad-div parameter for stable mixed finite element spaces and for stable equal order spaces like the MINI element.

The remaining part of this paper is organized as follows. In Section 2, we introduce the requisite functional spaces and the assumptions on the domain and on the given data. Then the positivity property of the kernel of the memory term and the Gronwall's lemma, both continuous and discrete versions, are mentioned there. In Section 3, the semidiscrete formulation and error analysis of the stabilized scheme is carried out, and in Section 4 backward Euler method is applied to the stabilized system. Finally, in Section 5, some numerical examples are given which conform with our theoretical results. We also obtain numerically suitable values of the grad-div parameter for the Oldroyd model of order one that minimizes velocity and pressure errors. Throughout this paper, we will use C as a generic constant, which depends on the given data and not on spatial and time discretization parameters. We note that C may grow exponentially with time, but it does not depend on inverse powers of μ.

2. Preliminaries

For our subsequent use, we denote by boldface letters the $\mathbb{R}^2$-valued function space such as $\mathbf{H}_0^1 = [H_0^1(\Omega)]^2$, $\mathbf{L}^2 = [L^2(\Omega)]^2$ and $\mathbf{H}^m = [H^m(\Omega)]^2$. We denote by $\|\cdot\|_i$ the usual norm on the Sobolev space $\mathbf{H}^i$, for $i = 1, 2$ and $(\cdot,\cdot)$ and $\|\cdot\|$ be the inner product and norm on L^2 or $\mathbf{L}^2$. The norm on the space of essentially bounded functions $\mathbf{L}^\infty(\Omega)$ will be denoted by $\|\cdot\|_\infty$. The space $\mathbf{H}_0^1$ is equipped with the norm

$$\|\nabla \mathbf{v}\| = \Big(\sum_{i,j=1}^{2}(\partial_j v_i, \partial_j v_i)\Big)^{1/2} = \Big(\sum_{i=1}^{2}(\nabla v_i, \nabla v_i)\Big)^{1/2}.$$

We denote by $\mathbf{J}_1$ and $\mathbf{J}$, the divergence free subspaces of $\mathbf{H}_0^1$ and $\mathbf{L}^2$, respectively.

$$\mathbf{J}_1 = \{\boldsymbol{\phi} \in \mathbf{H}_0^1 : \nabla \cdot \boldsymbol{\phi} = 0\},$$
$$\mathbf{J} = \{\boldsymbol{\phi} \in \mathbf{L}^2 : \nabla \cdot \boldsymbol{\phi} = 0 \ \text{ in } \ \Omega, \ \boldsymbol{\phi} \cdot \mathbf{n}|_{\partial\Omega} = 0 \ \text{ holds weakly}\},$$

where $\mathbf{n}$ is the outward normal to the boundary $\partial\Omega$ and $\boldsymbol{\phi} \cdot \mathbf{n}|_{\partial\Omega} = 0$ should be understood in the sense of trace in $\mathbf{H}^{-1/2}(\partial\Omega)$. Let $H^m/\mathbb{R}$ be the quotient space with norm $\|\phi\|_{H^m/\mathbb{R}} = \inf_{c\in\mathbb{R}} \|\phi + c\|_m$. For $m = 0$, it is denoted by $L^2/\mathbb{R}$. For any Banach space X, let $L^p(0,T;X)$ denote the space of measurable X-valued functions $\boldsymbol{\phi}$ on $(0,T)$ such that

$$\int_0^T \|\boldsymbol{\phi}(t)\|_X^p \, dt < \infty, \quad \text{if } 1 \le p < \infty, \quad \text{and} \quad \operatorname*{ess\,sup}_{0<t<T} \|\boldsymbol{\phi}(t)\|_X < \infty, \quad \text{if } p = \infty.$$

The dual space of $H^m(\Omega)$, denoted by $H^{-m}(\Omega)$, is defined as the completion of $C^\infty(\bar{\Omega})$ with respect to the norm

$$\|\phi\|_{-m} := \sup\left\{\frac{(\phi,\psi)}{\|\psi\|_m} : \psi \in H^m(\Omega), \|\psi\|_m \neq 0\right\}.$$

The following Sobolev's embedding [2] will be used for our analysis: For $1 \le p \le d/s$, let q be such that $\frac{1}{q} = \frac{1}{p} - \frac{s}{d}$, then there exists a constant C independent of s, such that

$$\|v\|_{L^{q'}(\Omega)} \le C\|v\|_{W^{s,p}(\Omega)}, \quad \frac{1}{q'} \ge \frac{1}{q}, \quad v \in W^{s,p}(\Omega).$$

If $p > \frac{d}{s}$ the above result is valid for $q' = \infty$. In our case, we consider $d = 2$. The similar embedding inequality holds for vector-valued functions. Throughout this paper, we make the following assumption:
(**A1**) For $\mathbf{g} \in \mathbf{H}^{m-1}$ with $m \ge 1$, let the unique pair of solutions $\{\mathbf{v} \in \mathbf{J}_1, q \in L^2/\mathbb{R}\}$ for the steady state Stokes problem

$$-\mu\Delta\mathbf{v} + \nabla q = \mathbf{g}, \quad \nabla \cdot \mathbf{v} = 0 \ \text{ in } \Omega; \quad \mathbf{v}|_{\partial\Omega} = 0,$$

satisfy the following regularity result [27]:

$$\mu\|\mathbf{v}\|_{m+1} + \|q\|_{H^m/\mathbb{R}} \le C\|\mathbf{g}\|_{m-1}.$$

We first note here that (**A1**) implies (see [26])

$$\|\mathbf{v}\|_2 \le C\|\tilde{\Delta}\mathbf{v}\|, \quad \forall \mathbf{v} \in \mathbf{J}_1 \cap \mathbf{H}^2,$$
$$\|\mathbf{v}\| \le \lambda_1^{-1/2}\|\mathbf{v}\|_1, \quad \mathbf{v} \in \mathbf{H}_0^1,$$
$$\|\mathbf{v}\|_1 \le \lambda_1^{-1/2}\|\mathbf{v}\|_2, \quad \mathbf{v} \in \mathbf{J}_1 \cap \mathbf{H}^2,$$

where $\tilde{\Delta} = P\Delta$, $\tilde{\Delta} : \mathbf{J}_1 \cap \mathbf{H}^2 \subset \mathbf{J} \to \mathbf{J}$ is the Stokes operator and P is the orthogonal projection of $\mathbf{L}^2$ onto $\mathbf{J}$. Here, $\lambda_1 > 0$ is the least positive eigenvalue of $\tilde{\Delta}$.

We will subsequently use the Gagliardo-Nirenberg inequality [28]

$$\|\boldsymbol{\phi}\|_{L^p} \le C\|\boldsymbol{\phi}\|^{2/p}\|\nabla\boldsymbol{\phi}\|^{1-2/p}, \quad \forall\ \boldsymbol{\phi} \in \mathbf{H}_0^1, \tag{2.1}$$

where $2 \le p < \infty$ and $C = C(p,\Omega)$. Also, we will consider the Agmon's inequality [28]

$$\|\boldsymbol{\phi}\|_{L^\infty} \le C\|\boldsymbol{\phi}\|^{1/2}\|\Delta\boldsymbol{\phi}\|^{1/2}, \quad \forall\ \boldsymbol{\phi} \in \mathbf{H}^2, \tag{2.2}$$

where $C = C(\Omega)$.

Remark 2.1. We will use the discrete version of the above two inequalities with constants uniform in the discretizing parameter h, following [28].

We now make the following assumption about the given data for the problem (1.1)-(1.3).
(**A2**) The external force $\mathbf{f}$ satisfy for some $M_0 > 0$ and for $0 < T \leq \infty$

$$\mathbf{f}, \mathbf{f}_t \in L^\infty(0,T;\mathbf{H}^m) \quad \text{with} \sup_{0<t<T} \left\{ \|\mathbf{f}\|_m, \|\mathbf{f}_t\|_m \right\} \leq M_0, \text{ for some integer } m \geq 0.$$

Before going into the details, we define the continuous bilinear form $a(\cdot,\cdot)$ on $\mathbf{H}_0^1 \times \mathbf{H}_0^1$ by

$$a(\mathbf{v},\mathbf{w}) = (\nabla \mathbf{v}, \nabla \mathbf{w}), \quad \forall\ \mathbf{v},\mathbf{w} \in \mathbf{H}_0^1,$$

and the continuous trilinear form $b(\cdot,\cdot,\cdot)$ on $\mathbf{H}_0^1 \times \mathbf{H}_0^1 \times \mathbf{H}_0^1$ by

$$\begin{aligned} b(\mathbf{v},\mathbf{w},\boldsymbol{\phi}) &= ((\mathbf{v}\cdot\nabla)\mathbf{w},\boldsymbol{\phi}) + \frac{1}{2}((\nabla\cdot\mathbf{v})\mathbf{w},\boldsymbol{\phi}) \\ &= \frac{1}{2}((\mathbf{v}\cdot\nabla)\mathbf{w},\boldsymbol{\phi}) - \frac{1}{2}((\mathbf{v}\cdot\nabla)\boldsymbol{\phi},\mathbf{w}), \quad \forall\ \mathbf{v},\mathbf{w},\boldsymbol{\phi} \in \mathbf{H}_0^1. \end{aligned} \tag{2.3}$$

It is clearly seen that

$$b(\mathbf{v},\mathbf{w},\boldsymbol{\phi}) = -b(\mathbf{v},\boldsymbol{\phi},\mathbf{w}), \quad \forall\ \mathbf{v},\mathbf{w},\boldsymbol{\phi} \in \mathbf{H}_0^1. \tag{2.4}$$

In particular

$$b(\mathbf{v},\mathbf{w},\mathbf{w}) = 0, \quad \forall\ \mathbf{v},\mathbf{w} \in \mathbf{H}_0^1. \tag{2.5}$$

Let us introduce the weak formulation of (1.1)-(1.3): To find a pair of functions $\{\mathbf{u}(t), p(t)\} \in \mathbf{H}_0^1 \times L^2/\mathbb{R},\ t > 0$ such that for $\boldsymbol{\phi} \in \mathbf{H}_0^1,\ \chi \in L^2$

$$\left.\begin{aligned} &(\mathbf{u}_t,\boldsymbol{\phi}) + \mu a(\mathbf{u},\boldsymbol{\phi}) + b(\mathbf{u},\mathbf{u},\boldsymbol{\phi}) + \textstyle\int_0^t \beta(t-s)a(\mathbf{u}(s),\boldsymbol{\phi})\ ds - (p,\nabla\cdot\boldsymbol{\phi}) = (\mathbf{f},\boldsymbol{\phi}), \\ &(\nabla\cdot\mathbf{u},\chi) = 0. \end{aligned}\right\} \tag{2.6}$$

Equivalently, find $\mathbf{u}(t) \in \mathbf{J}_1,\ t > 0$ such that

$$(\mathbf{u}_t,\boldsymbol{\phi}) + \mu a(\mathbf{u},\boldsymbol{\phi}) + b(\mathbf{u},\mathbf{u},\boldsymbol{\phi}) + \int_0^t \beta(t-s)a(\mathbf{u}(s),\boldsymbol{\phi})ds = (\mathbf{f},\boldsymbol{\phi}), \quad \forall \boldsymbol{\phi} \in \mathbf{J}_1. \tag{2.7}$$

For the existence and uniqueness of the problem (2.6) and (2.7), we refer to [21]. For the regularity of the solutions $\mathbf{u}$ and p, we make the following assumptions depending on whether the initial velocity $\mathbf{u}_0$ is $\mathbf{H}^m$-smooth ($m > 2$) or $\mathbf{H}^2$-smooth:
(A3) Let us assume that $\mathbf{u}_0 \in \mathbf{H}_0^1 \cap \mathbf{H}^{\max\{2,m\}}$ is $\mathbf{H}^m$-smooth and the solution pair $(\mathbf{u}, p)$ of (2.6) satisfies

$$\begin{aligned} &\mathbf{u} \in L^2(0,T;\mathbf{H}^{m+1}) \cap L^2(0,T;(W^{1,\infty}(\Omega))^2) \cap L^\infty(0,T;\mathbf{H}^m), \\ &p \in L^2(0,T;H^m/\mathbb{R}) \cap L^\infty(0,T;H^{m-1}/\mathbb{R}) \end{aligned}$$

for all $m \geq 1$. Further, there exists a positive constant C that does not depend on the inverse power of μ such that for all $m \geq 1$, the following hold:

$$\max_{0\leq t\leq T} \left(\|\mathbf{u}(t)\|_m^2 + \|p(t)\|_{H^{m-1}/\mathbb{R}}^2 \right) \leq C, \quad \int_0^t \|\nabla \mathbf{u}(s)\|_\infty^2 ds \leq Ct,$$

$$e^{-2\alpha t}\int_0^t e^{2\alpha s}\Big(\|\mathbf{u}(s)\|_{m+1}^2+\|\mathbf{u}_s(s)\|_{m-1}^2+\|p(s)\|_{H^m/\mathbb{R}}^2\Big)\,ds\le C.$$

(A3′) Let us assume that the initial data $\mathbf{u}_0\in\mathbf{H}_0^1\cap\mathbf{H}^2$ is $\mathbf{H}^2$-smooth and the solution pair $(\mathbf{u},p)$ of (2.6) satisfies

$$\begin{aligned}&(\tau(t))^{m-2}\mathbf{u}\in L^2(0,T;\mathbf{H}^{m+1})\cap L^\infty(0,T;\mathbf{H}^m),\ \mathbf{u}\in L^2(0,T;(W^{1,\infty}(\Omega))^2),\\&(\tau(t))^{m-2}p\in L^2(0,T;H^m/\mathbb{R}),\end{aligned}$$

for $m\ge 2$, where $\tau(t)=\min\{1,t\}$ and for $m=1$,

$$\mathbf{u}\in L^2(0,T;\mathbf{H}^2)\cap L^2(0,T;(W^{1,\infty}(\Omega))^2)\cap L^\infty(0,T;\mathbf{H}^1),\ p\in L^2(0,T;H^1/\mathbb{R}).$$

Further, there exists a positive constant C that does not depend on the inverse power of μ such that, the following hold: For $m=1$,

$$\int_0^t\|\nabla\mathbf{u}(s)\|_\infty^2ds\le Ct,\quad \max_{0\le t\le T}\|\mathbf{u}(t)\|_1^2+e^{-2\alpha t}\int_0^t e^{2\alpha s}\|\mathbf{u}(s)\|_2^2ds\le C.$$

For $m\ge 2$, and for $\tau(t)=\min\{1,t\}$

$$\begin{aligned}&\max_{0\le t\le T}(\tau(t))^{m-2}\Big(\|\mathbf{u}(t)\|_m^2+\|p(t)\|_{H^{m-1}/\mathbb{R}}^2\Big)\le C,\\&e^{-2\alpha t}\int_0^t e^{2\alpha s}(\tau(s))^{m-2}\Big(\|\mathbf{u}(s)\|_{m+1}^2+\|\mathbf{u}_s(s)\|_{m-1}^2+\|p(s)\|_{H^m/\mathbb{R}}^2\Big)\,ds\le C.\end{aligned}$$

Note that, the assumptions (**A3**) and (**A3′**) are coincide for the case $m=1$ and 2.

Before we move to the next section, we present below a few lemmas which will be used in our subsequent analysis. First one deals with the positivity of the kernel β. The result is borrowed from [40, Lemma 2.1].

Lemma 2.1. *For arbitrary $\alpha>0$, $t^*>0$ and $\phi\in L^2(0,t^*)$, the following positive definite property holds*

$$\int_0^{t^*}\Big(\int_0^t\exp\left[-\alpha(t-s)\right]\phi(s)\,ds\Big)\phi(t)\,dt\ge 0.$$

Second and third Lemmas are on Gronwall's inequality.

Lemma 2.2 (Gronwall's Lemma)**.** *Let g,h,y be three locally integrable non-negative functions on the time interval $[0,\infty)$ such that for all $t\ge 0$*

$$y(t)+G(t)\le C+\int_0^t h(s)\ ds+\int_0^t g(s)y(s)\ ds,$$

where $G(t)$ is a non-negative function on $[0,\infty)$ and $C\ge 0$ is a constant. Then,

$$y(t)+G(t)\le\Big(C+\int_0^t h(s)\ ds\Big)\exp\Big(\int_0^t g(s)\ ds\Big).$$

Lemma 2.3 (discrete Gronwall's Lemma [27])**.** *Let k,B and $\{a_i,b_i,c_i,d_i\}_{i\in\mathbb{N}}$ be non-negative numbers such that*

$$a_n+k\sum_{i=1}^n b_i\le B+k\sum_{i=1}^n c_i+k\sum_{i=1}^n d_ia_i,\ \ n\ge 1. \tag{2.8}$$

Suppose that $kd_i \le 1$, *for all* i. *Set* $\gamma_i = (1 - kd_i)^{-1}$. *Then,*

$$a_n + k\sum_{i=1}^{n} b_i \le \Big\{B + k\sum_{i=1}^{n} c_i\Big\} \exp\Big(k\sum_{i=1}^{n}\gamma_i d_i\Big). \tag{2.9}$$

If the last sum of (2.8) extends only up to $n-1$, *then the estimate (2.9) holds for all* $k > 0$, *with* $\gamma_i \equiv 1$.

Remark 2.2. Whenever we use discrete Gronwall's Lemma, it restricts the time step size k.

3. Galerkin finite element method

In this section, we consider the finite element Galerkin approximations to the problem (1.1)-(1.3) with grad-div stabilization. From now on, we denote h, with $0 < h < 1$, to be a real positive spatial discretization parameter, tending to zero. Let $\mathcal{T}_h$ be a finite decomposition of mesh size h, of the polygonal domain $\bar{\Omega}$ into closed subsets, triangles, or quadrilaterals in two dimensions. The decomposition $\mathcal{T}_h$ is assumed to be "face to face" and satisfy a "uniform size" condition:

Any two elements of $\mathcal{T}_h$ *meet only in entire common sides or in vertices. Each element of* $\mathcal{T}_h$ *contains a circle of radius* $\kappa_1 h$ *and it's contained in a circle of radius* $\kappa_2 h$, *these constant* κ_1, κ_2 *being independent of* h.

Let $\mathbf{H}_h$ and L_h be two families of finite element spaces, finite-dimensional subspaces of $\mathbf{H}_0^1$ and $L^2/\mathbb{R}$, respectively, approximating the velocity vector and the pressure. It is assumed that the spaces $(\mathbf{H}_h,\, L_h)$ are of the form $(\mathbf{P}_k, P_{k-1})$ where $\mathbf{P}_k$ comprises of piecewise polynomial of degree at most $k, k > 1$. [However for $k = 1$, we consider the mini element $(\mathbf{P}_1 b, P_1)$ where $\mathbf{P}_1 b$ is the $\mathbf{P}_1$ space with bubble enrichment.]

Assume that the following approximation properties are satisfied for the spaces $\mathbf{H}_h$ and L_h:
(**B1**) For each $\mathbf{w} \in \mathbf{H}_0^1 \cap \mathbf{H}^{k+1}$ and $q \in H^k/\mathbb{R}$ with $k \ge 1$, then there exist approximations $i_h w \in \mathbf{H}_h$ and $j_h q \in L_h$ such that for all $0 \le j \le k$

$$\|\mathbf{w} - i_h\mathbf{w}\| + h\|\nabla(\mathbf{w} - i_h\mathbf{w})\| \le Ch^{j+1}\|\mathbf{w}\|_{j+1}, \quad \|q - j_h q\| \le Ch^j\|q\|_j. \tag{3.1}$$

Further, we will assume that the meshes are quasi-uniform and the following inverse hypothesis holds for $\mathbf{v}_h \in \mathbf{H}_h$, see [14, Theorem 3.2.6]

$$\|\mathbf{v}_h\|_{W^{m,p}(K)^d} \le Ch^{n-m-d(\frac{1}{q}-\frac{1}{p})}\|\mathbf{v}_h\|_{W^{n,q}(K)^d}, \tag{3.2}$$

where $0 \le n \le m \le 1$, $0 \le q \le p \le \infty$, h be the diameter of the mesh cell $K \in \mathcal{T}_h$ and $\|\cdot\|_{W^{m,p}(K)^d}$ is the norm in Sobolev space $W^{m,p}(K)^d$.

Now, we consider the discrete analogue of the weak formulations (1.1)-(1.3) with a grad-div stabilization term: Find $(\mathbf{u}_h, p_h)$ in $\mathbf{H}_h \times L_h$ satisfying

$$\left.\begin{aligned} &(\mathbf{u}_{ht}, \boldsymbol{\phi}_h) + \mu a(\mathbf{u}_h, \boldsymbol{\phi}_h) + b(\mathbf{u}_h, \mathbf{u}_h, \boldsymbol{\phi}_h) + \textstyle\int_0^t \beta(t-\tau) a(\mathbf{u}_h(\tau), \boldsymbol{\phi}_h)\, d\tau \\ &-(p_h, \nabla\cdot\boldsymbol{\phi}_h) + \rho(\nabla\cdot\mathbf{u}_h, \nabla\cdot\boldsymbol{\phi}_h) = (\mathbf{f}, \boldsymbol{\phi}_h), \quad \forall\ \boldsymbol{\phi}_h \in \mathbf{H}_h, \\ &(\nabla\cdot\mathbf{u}_h, \chi_h) = 0, \quad \forall\ \chi_h \in L_h, \end{aligned}\right\} \tag{3.3}$$

where $\rho \geq 0$ is the stabilization parameter and $\mathbf{u}_{0h} \in \mathbf{H}_h$ is suitable approximation of $\mathbf{u}_0 \in \mathbf{J}_1$.

Let us consider the associated weekly divergence-free subspace $\mathbf{J}_h$ of the discrete space $\mathbf{H}_h$ as

$$\mathbf{J}_h = \{\mathbf{v}_h \in \mathbf{H}_h : (\chi_h, \nabla \cdot \mathbf{v}_h) = 0, \forall \chi_h \in L_h\}.$$

Note that the space $\mathbf{J}_h$ is not a subspace of $\mathbf{J}_1$. So, we now introduce an equivalent Galerkin approximation in the space $\mathbf{J}_h$ as: Find $\mathbf{u}_h(t) \in \mathbf{J}_h$ such that $\mathbf{u}_h(0) = \mathbf{u}_{0h}$ and for $t > 0$

$$\begin{aligned}(\mathbf{u}_{ht}, \boldsymbol{\phi}_h) + \mu a(\mathbf{u}_h, \boldsymbol{\phi}_h) + b(\mathbf{u}_h, \mathbf{u}_h, \boldsymbol{\phi}_h) + \int_0^t \beta(t-\tau) a(\mathbf{u}_h(\tau), \boldsymbol{\phi}_h)\, d\tau \\ + \rho(\nabla \cdot \mathbf{u}_h, \nabla \cdot \boldsymbol{\phi}_h) = (\mathbf{f}, \boldsymbol{\phi}_h), \quad \forall\, \boldsymbol{\phi}_h \in \mathbf{J}_h.\end{aligned} \tag{3.4}$$

Below, we present *a priori* estimate for the discrete solution.

Lemma 3.1. *Let the assumption* (**A1**) *hold. Then, the following stability estimate holds for the discrete velocity for all* $0 \leq t \leq T,\ T > 0$

$$\begin{aligned}&\|\mathbf{u}_h(t)\|^2 + 2e^{-2\alpha t} \int_0^t e^{2\alpha s} \left(\mu \|\nabla \mathbf{u}_h(s)\|^2 + \rho \|\nabla \cdot \mathbf{u}_h(s)\|^2\right) ds \\ &\leq \left(e^{-2\alpha t}\|\mathbf{u}_{0h}\|^2 + \frac{\|\mathbf{f}\|_\infty^2}{2\alpha}\right) e^{(1+2\alpha)t},\end{aligned}$$

where $\|\mathbf{f}\|_\infty = \sup_{0<t<T} \|\mathbf{f}(t)\|$.

Proof. Choose $\boldsymbol{\phi}_h = \mathbf{u}_h(t)$ in (3.4) and use (2.5) to obtain

$$\frac{1}{2}\frac{d}{dt}\|\mathbf{u}_h\|^2 + \mu\|\nabla \mathbf{u}_h\|^2 + \rho\|\nabla \cdot \mathbf{u}_h\|^2 + \int_0^t \beta(t-\tau) a(\mathbf{u}_h(\tau), \mathbf{u}_h)\, d\tau \leq (\mathbf{f}, \mathbf{u}_h).$$

We multiply both sides by $2e^{2\alpha t}$ and integrate with respect to time from 0 to t. Then, the use of the Cauchy-Schwarz inequality with the Young's inequality yields

$$\begin{aligned}&e^{2\alpha t}\|\mathbf{u}_h(t)\|^2 + 2\int_0^t e^{2\alpha s}\left(\mu\|\nabla \mathbf{u}_h(s)\|^2 + \rho\|\nabla \cdot \mathbf{u}_h(s)\|^2\right) ds \\ &+ 2\int_0^t e^{2\alpha s} \int_0^s \beta(s-\tau) a(\mathbf{u}_h(\tau), \mathbf{u}_h(s))\, d\tau\, ds \\ &\leq \|\mathbf{u}_h(0)\|^2 + \int_0^t e^{2\alpha s}\|\mathbf{f}\|^2 ds + (1+2\alpha)\int_0^t e^{2\alpha s}\|\mathbf{u}_h(s)\|^2 ds.\end{aligned}$$

The double integration term on the left-hand side is positive due to Lemma 2.1; hence, we drop it. Then, we use the Gronwall's lemma to arrive at

$$\begin{aligned}&e^{2\alpha t}\|\mathbf{u}_h(t)\|^2 + 2\int_0^t e^{2\alpha s}\left(\mu\|\nabla \mathbf{u}_h(s)\|^2 + \rho\|\nabla \cdot \mathbf{u}_h(s)\|^2\right) ds \\ &\leq \left(\|\mathbf{u}_{0h}\|^2 + \frac{\|\mathbf{f}\|_\infty^2}{2\alpha}(e^{2\alpha t} - 1)\right) e^{(1+2\alpha)t}.\end{aligned}$$

We multiply both sides by $e^{-2\alpha t}$ to complete the rest of the proof. □

Lemma 3.1 helps us to prove the local existence of the solution of (3.4). Once we have the solution of (3.4), then using this, we can easily prove the existence of the solutions of (3.3). The proof is quite similar to that of [40]; hence we skip it. The uniqueness of the pressure is obtained on the quotient space L_h/N_h, where

$$N_h = \{q_h \in L_h : (q_h, \nabla \cdot \boldsymbol{\phi}_h) = 0 \text{ for } \boldsymbol{\phi}_h \in \mathbf{H}_h\}.$$

The norm of L_h/N_h is given by

$$\|q_h\|_{L^2/N_h} = \inf_{\chi_h \in N_h} \|q_h + \chi_h\|.$$

Since $\mathbf{J}_h$ is finite-dimensional, the problem (3.4) leads to a system of nonlinear integro-differential equations with a stabilization term. For continuous dependence of the discrete pressure $p_h(t) \in L_h/N_h$ on the discrete velocity $\mathbf{u}_h(t) \in \mathbf{J}_h$, we assume the following discrete inf-sup (LBB) condition:

(**B2′**) For every $q_h \in L_h$, there exists a non-trivial function $\boldsymbol{\phi}_h \in \mathbf{H}_h$ such that

$$\inf_{q_h \in L_h} \sup_{\boldsymbol{\phi}_h \in \mathbf{H}_h} \frac{|(q_h, \nabla \cdot \boldsymbol{\phi}_h)|}{\|\nabla \boldsymbol{\phi}_h\| \|q_h\|_{L^2/N_h}} \geq C, \tag{3.5}$$

where the constant $C > 0$ is independent of h.

Moreover, we also assume that the following approximation property holds true for $\mathbf{J}_h$.

(**B2**) For every $\mathbf{w} \in \mathbf{J}_1 \cap \mathbf{H}^{k+1}$, there exists an approximation $r_h\mathbf{w} \in \mathbf{J}_h$ such that

$$\|\mathbf{w} - r_h\mathbf{w}\| + h\|\nabla(\mathbf{w} - r_h\mathbf{w})\| \leq Ch^{j+1}\|\mathbf{w}\|_{j+1}, \quad 0 \leq j \leq k. \tag{3.6}$$

We define L^2-projection $P_h : \mathbf{L}^2 \to \mathbf{J}_h$ satisfy the following properties for $0 \leq j \leq k$ [27]

$$\|\boldsymbol{\phi} - P_h\boldsymbol{\phi}\| + h\|\nabla(\boldsymbol{\phi} - P_h\boldsymbol{\phi})\| \leq Ch^{j+1}\|\boldsymbol{\phi}\|_{j+1}, \quad \forall\ \boldsymbol{\phi} \in \mathbf{J}_1(\Omega) \cap \mathbf{H}^{k+1}(\Omega). \tag{3.7}$$

Let us also consider the Lagrange interpolant $I_h\mathbf{u} \in \mathbf{H}_h$ of a continuous function $\mathbf{u}$ satisfying the following bounds (see [10, Theorem 4.4.4])

$$\|\mathbf{u} - I_h\mathbf{u}\|_{W^{m,p}(K)} \leq Ch^{n-m}\|\mathbf{u}\|_{W^{n,p}(K)}, \quad 0 \leq m \leq n \leq k+1, \tag{3.8}$$

where $n > \frac{2}{p}$ when $1 < p \leq \infty$ and $n \geq 2$ when $p = 1$.

We now define the discrete operator $\Delta_h : \mathbf{H}_h \to \mathbf{H}_h$ through the bilinear form $a(\cdot, \cdot)$ as

$$a(\mathbf{v}_h, \boldsymbol{\phi}_h) = (-\Delta_h\mathbf{v}_h, \boldsymbol{\phi}_h), \quad \forall\ \mathbf{v}_h, \boldsymbol{\phi}_h \in \mathbf{H}_h.$$

We also define the discrete Stokes operator $\tilde{\Delta}_h = P_h\Delta_h$ of $\tilde{\Delta} = P\Delta$. The restriction of $\tilde{\Delta}_h$ to $\mathbf{J}_h$ is invertible and its inverse is denoted as $\tilde{\Delta}_h^{-1}$. We recall the discrete Sobolev norms on $\mathbf{J}_h$ (see [27]): For $r \in \mathbb{R}$, we define

$$\|\mathbf{v}_h\|_r := \|(-\tilde{\Delta}_h)^{r/2}\mathbf{v}\|, \quad \mathbf{v}_h \in \mathbf{J}_h.$$

We note that $\|\mathbf{v}_h\|_0 = \|\mathbf{v}_h\|$ and $\|\mathbf{v}_h\|_1 = \|\nabla\mathbf{v}_h\|$. Also the norm $\|\tilde{\Delta}_h(\cdot)\|$ is equivalent to the norm $\|\cdot\|_2$ in $\mathbf{J}_h$ with constant independent of h.

We present below the error analysis due to the space discretization (time remains continuous). Our analysis will be divided into two parts based on the regularity of the given initial data. First, we consider $\mathbf{H}^m$-smooth initial data, that is, the initial velocity $\mathbf{u}_0 \in \mathbf{H}_0^1 \cap \mathbf{H}^{\max\{2,m\}}$, $m = k$, and then, we take $\mathbf{H}^2$-smooth initial data, that is, $\mathbf{u}_0 \in \mathbf{H}_0^1 \cap \mathbf{H}^2$.

3.1. Semidiscrete error estimate for $\mathbf{H}^m$-smooth data

In this section, we derive error bounds for the velocity and the pressure for the case when the exact solution remains regular as $t \to 0$; that is, the given data is as much regular as we need.

3.1.1. Error bounds for velocity

Since $\mathbf{J}_h$ is not a subspace of $\mathbf{J}_1$, the weak solution $\mathbf{u}$ of the Oldroyd model of order one satisfies for all $\boldsymbol{\phi}_h \in \mathbf{J}_h$

$$(\mathbf{u}_t, \boldsymbol{\phi}_h) + \mu a(\mathbf{u}, \boldsymbol{\phi}_h) + b(\mathbf{u}, \mathbf{u}, \boldsymbol{\phi}_h) + \int_0^t \beta(t-s) a(\mathbf{u}(s), \boldsymbol{\phi}_h) ds = (\mathbf{f}, \boldsymbol{\phi}) + (p, \nabla \cdot \boldsymbol{\phi}_h). \tag{3.9}$$

Define $\mathbf{e} = \mathbf{u} - \mathbf{u}_h$, then subtract (3.4) from (3.9) and use $\nabla \cdot \mathbf{u} = 0$ to obtain the following error equation

$$\begin{aligned}&(\mathbf{e}_t, \boldsymbol{\phi}_h) + \mu a(\mathbf{e}, \boldsymbol{\phi}_h) + \int_0^t \beta(t-s) a(\mathbf{e}(s), \boldsymbol{\phi}_h) ds + \rho(\nabla \cdot \mathbf{e}, \nabla \cdot \boldsymbol{\phi}_h) \\ =&(p, \nabla \cdot \boldsymbol{\phi}_h) + b(\mathbf{u}_h, \mathbf{u}_h, \boldsymbol{\phi}_h) - b(\mathbf{u}, \mathbf{u}, \boldsymbol{\phi}_h), \ \forall \boldsymbol{\phi}_h \in \mathbf{J}_h.\end{aligned} \tag{3.10}$$

Theorem 3.1. *Assume that* (**A1**)-(**A3**), (**B1**) *and* (**B2**) *hold. Let $\alpha > 0$ be such that $\mu - \left(\frac{\gamma}{\delta-\alpha}\right)^2 > 0$. Then, there exists a positive constant C that does not depend on the inverse power of μ, such that the following bounds hold for $t \in [0,T], T > 0$*

$$\|\mathbf{e}(t)\|^2 + \beta_1 e^{-2\alpha t} \int_0^t e^{2\alpha s} \|\nabla \mathbf{e}(s)\|^2 ds + \rho e^{-2\alpha t} \int_0^t e^{2\alpha s} \|\nabla \cdot \mathbf{e}(s)\|^2 ds \leq C h^{2k} e^{L(t)},$$

where, $\beta_1 = \mu - \left(\frac{\gamma}{\delta-\alpha}\right)^2 > 0$, and

$$L(t) = \int_0^t \left(2\alpha + 4\|\nabla \mathbf{u}(s)\|_\infty + (1 + \frac{4}{\rho})\|\mathbf{u}(s)\|_2^2\right) ds, \tag{3.11}$$

and C depends on

$$\|\mathbf{u}(t)\|_k^2 + e^{-2\alpha t} \int_0^t e^{2\alpha s} \left((\mu + 4\rho + 2)\|\mathbf{u}(s)\|_{k+1}^2 + \frac{4}{\rho}\|p(s)\|_k^2\right) ds. \tag{3.12}$$

Proof. Choose $\boldsymbol{\phi}_h = P_h \mathbf{e} = \mathbf{e} - (\mathbf{u} - P_h \mathbf{u})$ in (3.10) to arrive at

$$\begin{aligned}&\frac{1}{2}\frac{d}{dt}\|\mathbf{e}\|^2 + \mu\|\nabla \mathbf{e}\|^2 + \rho\|\nabla \cdot \mathbf{e}\|^2 + \int_0^t \beta(t-\tau) a(\mathbf{e}(\tau), \mathbf{e}) d\tau \\ =& (\mathbf{e}_t, \mathbf{u} - P_h \mathbf{u}) + \mu a(\mathbf{e}, \mathbf{u} - P_h \mathbf{u}) + \rho(\nabla \cdot \mathbf{e}, \nabla \cdot (\mathbf{u} - P_h \mathbf{u})) \\ &+ \int_0^t \beta(t-\tau) a(\mathbf{e}(\tau), \mathbf{u} - P_h \mathbf{u}) d\tau + (p, \nabla \cdot P_h \mathbf{e}) - \Lambda(P_h \mathbf{e}),\end{aligned} \tag{3.13}$$

where

$$\Lambda(\boldsymbol{\phi}_h) = b(\mathbf{u}, \mathbf{u}, \boldsymbol{\phi}_h) - b(\mathbf{u}_h, \mathbf{u}_h, \boldsymbol{\phi}_h) = b(\mathbf{u}, \mathbf{e}, \boldsymbol{\phi}_h) + b(\mathbf{e}, \mathbf{u}, \boldsymbol{\phi}_h) - b(\mathbf{e}, \mathbf{e}, \boldsymbol{\phi}_h).$$

Now, using the definition of P_h, we tackle the first term on the right hand side of (3.13) as

$$\begin{aligned}(\mathbf{e}_t, \mathbf{u}-P_h\mathbf{u}) &= (\mathbf{u}_t - P_h\mathbf{u}_t + P_h\mathbf{u}_t - \mathbf{u}_{ht}, \mathbf{u}-P_h\mathbf{u})\\ &= (\mathbf{u}_t - P_h\mathbf{u}_t, \mathbf{u}-P_h\mathbf{u})\\ &= \frac{1}{2}\frac{d}{dt}\|\mathbf{u}-P_h\mathbf{u}\|^2. \end{aligned}\tag{3.14}$$

An application of the Cauchy-Schwarz inequality and the Young's inequality with (3.7) leads to

$$\begin{aligned}\mu|a(\mathbf{e}, \mathbf{u}-P_h\mathbf{u})| &\le \mu\|\nabla\mathbf{e}\|\|\nabla(\mathbf{u}-P_h\mathbf{u})\|\\ &\le C\mu h^k\|\mathbf{u}\|_{k+1}\|\nabla\mathbf{e}\|\\ &\le \frac{C\mu}{2}h^{2k}\|\mathbf{u}\|_{k+1}^2 + \frac{\mu}{2}\|\nabla\mathbf{e}\|^2. \end{aligned}\tag{3.15}$$

Use of the Cauchy-Schwarz inequality and the Young's inequality with (3.7) and $\|\nabla\cdot\boldsymbol{\phi}\| \le C\|\nabla\boldsymbol{\phi}\|$ yield

$$\begin{aligned}\rho|(\nabla\cdot\mathbf{e}, \nabla\cdot(\mathbf{u}-P_h\mathbf{u}))| &\le C\rho\|\nabla\cdot\mathbf{e}\|\|\nabla(\mathbf{u}-P_h\mathbf{u})\|\\ &\le 2C\rho h^{2k}\|\mathbf{u}\|_{k+1}^2 + \frac{\rho}{8}\|\nabla\cdot\mathbf{e}\|^2. \end{aligned}\tag{3.16}$$

The integration term on the right-hand side can be estimated as

$$\begin{aligned}\int_0^t \beta(t-\tau)a(\mathbf{e}(\tau), \mathbf{u}-P_h\mathbf{u})d\tau &\le \left(\int_0^t \beta(t-\tau)\|\nabla\mathbf{e}(\tau)\|d\tau\right)\|\nabla(\mathbf{u}-P_h\mathbf{u})\|\\ &\le Ch^k\left(\int_0^t \beta(t-\tau)\|\nabla\mathbf{e}(\tau)\|d\tau\right)\|\mathbf{u}\|_{k+1} \qquad (3.17)\\ &\le \frac{C}{2}h^{2k}\|\mathbf{u}\|_{k+1}^2 + \frac{1}{2}\left(\int_0^t \beta(t-\tau)\|\nabla\mathbf{e}(\tau)\|d\tau\right)^2. \end{aligned}$$

A use of discrete incompressibility condition, that is, $(j_h p, \nabla\cdot P_h\mathbf{e} = 0)$, with the Cauchy-Schwarz inequality and the approximation property (3.1) yields

$$\begin{aligned}|(p, \nabla\cdot P_h\mathbf{e})| &= |(p - j_h p, \nabla\cdot P_h\mathbf{e})|\\ &\le Ch^k\|p\|_k\|\nabla\cdot\mathbf{e}\|\\ &\le \frac{2C}{\rho}h^{2k}\|p\|_k^2 + \frac{\rho}{8}\|\nabla\cdot\mathbf{e}\|^2. \end{aligned}\tag{3.18}$$

Using (2.5), we can rewrite the nonlinear terms as

$$\begin{aligned}|\Lambda(P_h\mathbf{e})| \le\ &|b(\mathbf{u}, \mathbf{e}, \mathbf{u}-P_h\mathbf{u})| + |b(\mathbf{e}, \mathbf{u}, \mathbf{e})|\\ &+ |b(\mathbf{e}, \mathbf{u}, \mathbf{u}-P_h\mathbf{u})| + |b(\mathbf{e}, \mathbf{e}, \mathbf{u}-P_h\mathbf{u})|. \end{aligned}\tag{3.19}$$

We use (2.4) and (2.3) with the Hölder's inequality, the Gagliardo-Nirenberg inequality (2.1), the Agmon's inequality (2.2), the Young's inequality, the continuous divergence constraint $\nabla\cdot\mathbf{u} = 0$ and (3.7) to bound the first term on the right-hand side of (3.19) as

$$|b(\mathbf{u}, \mathbf{e}, \mathbf{u}-P_h\mathbf{u})| = |b(\mathbf{u}, \mathbf{u}-P_h\mathbf{u}, \mathbf{e})|$$

$$
\begin{aligned}
&= |((\mathbf{u}\cdot\nabla)(\mathbf{u}-P_h\mathbf{u}),\mathbf{e}) + \frac{1}{2}((\nabla\cdot\mathbf{u})(\mathbf{u}-P_h\mathbf{u}),\mathbf{e})| \\
&\leq \|\mathbf{u}\|_\infty\|\nabla(\mathbf{u}-P_h\mathbf{u})\|\|\mathbf{e}\| + \frac{1}{2}\|\nabla\cdot\mathbf{u}\|_{L^4}\|\mathbf{u}-P_h\mathbf{u}\|_{L^4}\|\mathbf{e}\| \\
&\leq Ch^k\|\mathbf{e}\|\|\mathbf{u}\|_2\|\mathbf{u}\|_{k+1} \\
&\leq \frac{C}{2}h^{2k}\|\mathbf{u}\|_{k+1}^2 + \frac{C}{2}\|\mathbf{u}\|_2^2\|\mathbf{e}\|^2. \qquad (3.20)
\end{aligned}
$$

Third term on the right-hand side of (3.19) can also be estimated as follows:

$$
\begin{aligned}
|b(\mathbf{e},\mathbf{u},\mathbf{u}-P_h\mathbf{u})| &= |\frac{1}{2}((\mathbf{e}\cdot\nabla)\mathbf{u},\mathbf{u}-P_h\mathbf{u}) - \frac{1}{2}((\mathbf{e}\cdot\nabla)(\mathbf{u}-P_h\mathbf{u}),\mathbf{u})| \\
&\leq \frac{1}{2}(\|\mathbf{e}\|\|\nabla\mathbf{u}\|_{L^4}\|\mathbf{u}-P_h\mathbf{u}\|_{L^4} + \|\mathbf{e}\|\|\nabla(\mathbf{u}-P_h\mathbf{u})\|\|\mathbf{u}\|_\infty) \\
&\leq Ch^k\|\mathbf{e}\|\|\mathbf{u}\|_2\|\mathbf{u}\|_{k+1} \\
&\leq \frac{C}{2}h^{2k}\|\mathbf{u}\|_{k+1}^2 + \frac{C}{2}\|\mathbf{u}\|_2^2\|\mathbf{e}\|^2. \qquad (3.21)
\end{aligned}
$$

To bound the second term on the right-hand side of (3.19), use (2.3) with the Cauchy-Schwarz inequality and the Agmon's inequality (2.2) as

$$
\begin{aligned}
|b(\mathbf{e},\mathbf{u},\mathbf{e})| &\leq ((\mathbf{e}\cdot\nabla)\mathbf{u},\mathbf{e}) + \frac{1}{2}((\nabla\cdot\mathbf{e})\mathbf{u},\mathbf{e}) \\
&\leq \|\nabla\mathbf{u}\|_\infty\|\mathbf{e}\|^2 + \frac{1}{2}\|\nabla\cdot\mathbf{e}\|\|\mathbf{u}\|_\infty\|\mathbf{e}\| \\
&\leq C\left(\|\nabla\mathbf{u}\|_\infty + \frac{1}{\rho}\|\mathbf{u}\|_2^2\right)\|\mathbf{e}\|^2 + \frac{\rho}{8}\|\nabla\cdot\mathbf{e}\|^2. \qquad (3.22)
\end{aligned}
$$

For the last term on right hand side of (3.19), use (2.4) then doing similar as (3.22) to obtain

$$
\begin{aligned}
|b(\mathbf{e},\mathbf{e},\mathbf{u}-P_h\mathbf{u})| &= |b(\mathbf{e},\mathbf{u}-P_h\mathbf{u},\mathbf{e})| \\
&\leq C(\|\nabla(\mathbf{u}-P_h\mathbf{u})\|_\infty + \frac{1}{\rho}\|\mathbf{u}-P_h\mathbf{u}\|_\infty^2)\|\mathbf{e}\|^2 + \frac{\rho}{8}\|\nabla\cdot\mathbf{e}\|^2 \\
&\leq C(\|\nabla\mathbf{u}\|_\infty + \frac{1}{\rho}\|\mathbf{u}\|_2^2)\|\mathbf{e}\|^2 + \frac{\rho}{8}\|\nabla\cdot\mathbf{e}\|^2. \qquad (3.23)
\end{aligned}
$$

Inserting (3.14)-(3.23) in (3.13) and then multiplying both side by $e^{2\alpha t}$, we arrive at

$$
\begin{aligned}
&\frac{1}{2}\frac{d}{dt}e^{2\alpha t}\|\mathbf{e}\|^2 + \frac{\mu}{2}e^{2\alpha t}\|\nabla\mathbf{e}\|^2 + \frac{\rho}{2}e^{2\alpha t}\|\nabla\cdot\mathbf{e}\|^2 + e^{2\alpha t}\int_0^t\beta(t-\tau)a(\mathbf{e}(\tau),\mathbf{e})d\tau \\
\leq&\frac{1}{2}\frac{d}{dt}e^{2\alpha t}\|\mathbf{u}-P_h\mathbf{u}\|^2 - \alpha e^{2\alpha t}\|\mathbf{u}-P_h\mathbf{u}\|^2 \\
&+ Ch^{2k}e^{2\alpha t}\Big((\frac{\mu}{2}+2\rho+1)\|\mathbf{u}\|_{k+1}^2 + \frac{2}{\rho}\|p\|_k^2\Big) \\
&+ e^{2\alpha t}\Big(2\|\nabla\mathbf{u}\|_\infty + (\frac{1}{2}+\frac{2}{\rho})\|\mathbf{u}\|_2^2 + \alpha\Big)\|\mathbf{e}\|^2 \\
&+ \frac{1}{2}e^{2\alpha t}\Big(\int_0^t\beta(t-\tau)\|\nabla\mathbf{e}(\tau)\|d\tau\Big)^2. \qquad (3.24)
\end{aligned}
$$

First, we drop the second term on the right-hand side of (3.24) and then integrate with respect to time from 0 to t and use $\|\mathbf{e}(0)\| = \|\mathbf{u}(0) - P_h\mathbf{u}(0)\|$ to obtain

$$\begin{aligned}
&e^{2\alpha t}\|\mathbf{e}(t)\|^2 + \mu\int_0^t e^{2\alpha s}\|\nabla\mathbf{e}(s)\|^2 ds + \rho\int_0^t e^{2\alpha s}\|\nabla\cdot\mathbf{e}(s)\|^2 ds \\
&+ 2\int_0^t e^{2\alpha s}\int_0^s \beta(s-\tau)a(\mathbf{e}(\tau),\mathbf{e}(s))d\tau ds \\
\le\, & e^{2\alpha t}\|\mathbf{u}(t) - P_h\mathbf{u}(t)\|^2 \\
&+ Ch^{2k}\int_0^t e^{2\alpha s}\Big((\mu+4\rho+2)\|\mathbf{u}(s)\|_{k+1}^2 + \frac{4}{\rho}\|p(s)\|_k^2\Big)ds \\
&+ \int_0^t e^{2\alpha s}\Big(2\alpha + 4\|\nabla\mathbf{u}\|_\infty + (1+\frac{4}{\rho})\|\mathbf{u}\|_2^2\Big)\|\mathbf{e}(s)\|^2 ds \\
&+ \int_0^t e^{2\alpha s}\Big(\int_0^s \beta(s-\tau)\|\nabla\mathbf{e}(\tau)\|d\tau\Big)^2 ds. \qquad (3.25)
\end{aligned}$$

From Lemma 2.1, the double integration term on left-hand side is positive, so we can drop it and the double integration term on right-hand side can be bounded as similar as (4.2) of [40, page 761] as

$$\int_0^t e^{2\alpha s}\Big(\int_0^s \beta(s-\tau)\|\nabla\mathbf{e}(\tau)\|d\tau\Big)^2 ds \le \Big(\frac{\gamma}{\delta-\alpha}\Big)^2\int_0^t e^{2\alpha s}\|\nabla\mathbf{e}(s)\|^2 ds. \qquad (3.26)$$

Now, use (3.26) in (3.25) with $\beta_1 = \mu - \big(\frac{\gamma}{\delta-\alpha}\big)^2 > 0$ and use the Gronwall's lemma to conclude

$$\begin{aligned}
&e^{2\alpha t}\|\mathbf{e}(t)\|^2 + \beta_1\int_0^t e^{2\alpha s}\|\nabla\mathbf{e}(s)\|^2 ds + \rho\int_0^t e^{2\alpha s}\|\nabla\cdot\mathbf{e}(s)\|^2 ds \\
\le\, & Ch^{2k}e^{L(t)}\Big[e^{2\alpha t}\|\mathbf{u}(t)\|_k^2 + \int_0^t e^{2\alpha s}\Big((\mu+4\rho+2)\|\mathbf{u}(s)\|_{k+1}^2 + \frac{4}{\rho}\|p(s)\|_k^2\Big)ds\Big].
\end{aligned}$$

Multiply both sides by $e^{-2\alpha t}$, which completes the rest of the proof. □

Remark 3.1. In Theorem 3.1, such a choice of $\alpha > 0$ is possible under the assumption that $\mu > (\nu-\mu)^2$ and by choosing $\alpha < \delta\big(1 - \frac{\nu-\mu}{\sqrt{\mu}}\big)$.

Remark 3.2. From the assumption **(A3)**, it is clear that $L(t)$ defined on (3.11) is bounded by $C(t)$ and the quantity in (3.12) is also bounded by C, where C does not depend on μ^{-1}.

Remark 3.3. For stable mixed finite element spaces $(\mathbf{P}_k, P_{k-1})$, $k > 1$, the constant C of Theorem 3.1 does not depends on the inverse power of μ, but it depends on ρ and ρ^{-1}. This justifies the standard choice of grad-div stabilization parameter to be $\rho \approx 1$ (as for NSEs, see [37,38]). However, we have numerically verified that it depends on the mesh size, the type of mesh, the viscosity, and the finite element spaces as well. (Detailed discussion for Stokes and NSEs can be found in [3,29].)

For a pair of equal degree inf-sup stable finite element spaces like the MINI element $(\mathbf{P}_1 b, P_1)$, the constant C depends on

$$\|\mathbf{u}(t)\|_1^2 + e^{-2\alpha t}\int_0^t e^{2\alpha s}\left((\mu+4\rho+2)\|\mathbf{u}(s)\|_2^2 + \frac{4h^2}{\rho}\|p(s)\|_2^2\right)ds,$$

Then, we can choose $\rho \approx h^2$ or h, which gives us the optimal result. In other words, we can choose the stabilization parameter ρ in a range of h^2 to 1.

3.1.2. Error bounds for pressure

Theorem 3.2. *Let us assume that the hypothesis of the Lemma* 3.1 *holds true. Additionally, we assume that* $\mathbf{u}_t \in L^2(0,T;\mathbf{H}^{k-1})$, *then there exists a positive constant* C *independent of* μ^{-1}, *such that, for all* $t > 0$,

$$e^{-2\alpha t}\int_0^t e^{2\alpha s}\|(p-p_h)(s)\|^2_{L^2/N_h} ds \le Ch^{2k}e^{L(t)},$$

holds, where, $L(t)$ *is defined in (3.11) and* C *depends on the following*

$$\|\mathbf{u}(t)\|_k^2 + e^{-2\alpha t}\int_0^t e^{2\alpha s}\left(\|\mathbf{u}_s(s)\|^2_{k-1} + (\mu+4\rho+2)\|\mathbf{u}(s)\|^2_{k+1} + \frac{4}{\rho}\|p(s)\|_k^2\right) ds. \tag{3.27}$$

To achieve proof, we need some intermediate results. We start by splitting the pressure error $p - p_h$ as

$$\|p-p_h\| \le \|p - j_h p\| + \|j_h p - p_h\|. \tag{3.28}$$

We need to estimate the second term on the right-hand side of (3.28). Using (3.5), we rewrite it as

$$\begin{aligned}\|j_h p - p_h\|_{L^2/N_h} &\le C \sup_{\boldsymbol{\phi}_h \in \mathbf{H}_h/\{0\}} \left\{\frac{|(j_h p - p_h, \nabla\cdot\boldsymbol{\phi}_h)|}{\|\nabla\boldsymbol{\phi}_h\|}\right\} \\ &\le C\left(\|j_h p - p\| + \sup_{\boldsymbol{\phi}_h \in \mathbf{H}_h/\{0\}}\left\{\frac{|(p-p_h, \nabla\cdot\boldsymbol{\phi}_h)|}{\|\nabla\boldsymbol{\phi}_h\|}\right\}\right). \end{aligned} \tag{3.29}$$

The first term on the right-hand side of (3.29) can be estimated by using the approximation property (3.1). For the second term, we first look at the error equation in pressure obtained by subtracting (3.3) from (2.6):

$$\begin{aligned}(p-p_h, \nabla\cdot\boldsymbol{\phi}_h) = (\mathbf{e}_t, \boldsymbol{\phi}_h) + \mu a(\mathbf{e}, \boldsymbol{\phi}_h) + \int_0^t \beta(t-s)a(\mathbf{e}(s), \boldsymbol{\phi}_h)ds \\ + \rho(\nabla\cdot\mathbf{e}, \nabla\cdot\boldsymbol{\phi}_h) + \Lambda(\boldsymbol{\phi}_h),\end{aligned} \tag{3.30}$$

where

$$\Lambda(\boldsymbol{\phi}_h) = -b(\mathbf{u},\mathbf{u},\boldsymbol{\phi}_h) + b(\mathbf{u}_h,\mathbf{u}_h,\boldsymbol{\phi}_h) = -b(\mathbf{u}_h,\mathbf{e},\boldsymbol{\phi}_h) - b(\mathbf{e},\mathbf{u},\boldsymbol{\phi}_h), \quad \boldsymbol{\phi}_h \in \mathbf{H}_h.$$

Similar to (3.20) and (3.21), we bound the nonlinear terms as

$$|\Lambda(\boldsymbol{\phi}_h)| = C(\|\mathbf{u}\|_2 + \|\mathbf{u}_h\|_2)\|\mathbf{e}\|\|\nabla\boldsymbol{\phi}\|.$$

Since $\mathbf{u}$ is regular enough, $\mathbf{u}$ is continuous and hence, $\|I_h\mathbf{u}\|_2 \le C\|\mathbf{u}\|_2$, for some $C > 0$. Then, using (3.2), (3.8) and Lemma 3.1, one can find

$$\|\mathbf{u}_h\|_2 \le \|\mathbf{u}_h - I_h\mathbf{u}\|_2 + \|I_h\mathbf{u}\|_2 \le Ch^{-2}\|\mathbf{u}_h - I_h\mathbf{u}\| + C\|\mathbf{u}\|_2 \le C\|\mathbf{u}\|_3. \tag{3.31}$$

Apply the Cauchy-Schwarz inequality and (3.31) in (3.30) to arrive at

$$
\begin{aligned}
(p-p_h,\nabla\cdot\boldsymbol{\phi}_h) \leq & C\Big(\|\mathbf{e}_t\|_{-1;h}+\mu\|\nabla\mathbf{e}\|+\rho\|\nabla\cdot\mathbf{e}\|+\|\mathbf{u}\|_3\|\mathbf{e}\| \\
& +\int_0^t \beta(t-s)\|\nabla\mathbf{e}(s)\|ds\Big)\|\nabla\boldsymbol{\phi}_h\|,
\end{aligned}
\tag{3.32}
$$

where,

$$
\|\mathbf{e}_t\|_{-1;h}=\sup\left\{\frac{\langle\mathbf{e}_t,\boldsymbol{\phi}_h\rangle}{\|\nabla\boldsymbol{\phi}_h\|}:\boldsymbol{\phi}_h\in\mathbf{H}_h,\boldsymbol{\phi}_h\neq 0\right\}.
$$

Since all the estimate on right hand side in (3.32) are known except $\|\mathbf{e}_t\|_{-1;h}$, we now derive $\|\mathbf{e}_t\|_{-1;h}$. As $\mathbf{H}_h\subset\mathbf{H}_0^1$, we note that

$$
\begin{aligned}
\|\mathbf{e}_t\|_{-1;h} &=\sup\left\{\frac{\langle\mathbf{e}_t,\boldsymbol{\phi}_h\rangle}{\|\nabla\boldsymbol{\phi}_h\|}:\boldsymbol{\phi}_h\in\mathbf{H}_h,\boldsymbol{\phi}_h\neq 0\right\} \\
&\leq \sup\left\{\frac{\langle\mathbf{e}_t,\boldsymbol{\phi}\rangle}{\|\nabla\boldsymbol{\phi}\|}:\boldsymbol{\phi}\in\mathbf{H}_0^1,\boldsymbol{\phi}\neq 0\right\} \\
&=\|\mathbf{e}_t\|_{-1}.
\end{aligned}
$$

Lemma 3.2. *The error* $\mathbf{e}=\mathbf{u}-\mathbf{u}_h$ *satisfies for* $0<t<T$

$$
\begin{aligned}
\|\mathbf{e}_t\|_{-1} \leq & C\Big(h^k(\|\mathbf{u}_t\|_{k-1}+\|p\|_k)+\mu\|\nabla\mathbf{e}\|+\rho\|\nabla\cdot\mathbf{e}\|+\|\mathbf{u}\|_3\|\mathbf{e}\| \\
& +\int_0^t\beta(t-s)\|\nabla\mathbf{e}(s)\|ds\Big).
\end{aligned}
$$

Proof. For any $\boldsymbol{\psi}\in\mathbf{H}_0^1$, use the orthogonal projection $P_h:\mathbf{L}^2\to\mathbf{J}_h$, we obtain using (3.10) with $\boldsymbol{\phi}_h=P_h\boldsymbol{\psi}$

$$
\begin{aligned}
(\mathbf{e}_t,\boldsymbol{\psi}) =& (\mathbf{e}_t,\boldsymbol{\psi}-P_h\boldsymbol{\psi})+(\mathbf{e}_t,P_h\boldsymbol{\psi}) \\
=& (\mathbf{e}_t,\boldsymbol{\psi}-P_h\boldsymbol{\psi})-\mu a(\mathbf{e},P_h\boldsymbol{\psi})-\int_0^t\beta(t-s)a(\mathbf{e}(s),P_h\boldsymbol{\psi})ds+(p,\nabla\cdot P_h\boldsymbol{\psi}) \\
& -\rho(\nabla\cdot\mathbf{e},\nabla\cdot P_h\boldsymbol{\psi})-\Lambda(P_h\boldsymbol{\psi}).
\end{aligned}
\tag{3.33}
$$

Using the approximation property (3.7) of P_h, we find that

$$
(\mathbf{e}_t,\boldsymbol{\psi}-P_h\boldsymbol{\psi})=(\mathbf{u}_t-P_h\mathbf{u}_t,\boldsymbol{\psi}-P_h\boldsymbol{\psi})\leq Ch^k\|\mathbf{u}_t\|_{k-1}\|\nabla\boldsymbol{\psi}\|. \tag{3.34}
$$

Also, using discrete incompressibility condition and the approximation properties (3.1) and (3.7), we bound the pressure term as

$$
(p,\nabla\cdot P_h\boldsymbol{\psi})\leq(p-j_hp,\nabla\cdot P_h\boldsymbol{\psi})\leq Ch^k\|p\|_k\|\nabla\boldsymbol{\psi}\|. \tag{3.35}
$$

Now, substitute (3.34)-(3.35) in (3.33) and use (3.31) with $\boldsymbol{\phi}_h=P_h\boldsymbol{\psi}$ to obtain

$$
\begin{aligned}
(\mathbf{e}_t,\boldsymbol{\psi}) \leq & C\Big(h^k(\|\mathbf{u}_t\|_{k-1}+\|p\|_k)+\mu\|\nabla\mathbf{e}\|+\rho\|\nabla\cdot\mathbf{e}\|+\|\mathbf{u}\|_3\|\mathbf{e}\| \\
& +\int_0^t\beta(t-s)\|\nabla\mathbf{e}(s)\|ds\Big)\|\nabla\boldsymbol{\psi}\|.
\end{aligned}
$$

Therefore,

$$\begin{aligned}\|\mathbf{e}_t\|_{-1} \leq& \sup\left\{\frac{\langle \mathbf{e}_t, \boldsymbol{\phi}\rangle}{\|\nabla\boldsymbol{\phi}\|} : \boldsymbol{\phi}\in \mathbf{H}_0^1, \boldsymbol{\phi}\neq 0\right\}\\ \leq& C\Big(h^k(\|\mathbf{u}_t\|_{k-1}+\|p\|_k)+\mu\|\nabla\mathbf{e}\|+\rho\|\nabla\cdot\mathbf{e}\|+\|\mathbf{u}\|_3\|\mathbf{e}\|\\ &+\int_0^t \beta(t-s)\|\nabla\mathbf{e}(s)\|ds\Big),\end{aligned}$$

which completes the proof. □

Proof of the Theorem 3.2. From (3.28), (3.29), (3.32) and Lemma 3.2, we obtain

$$\begin{aligned}\|(p-p_h)\|^2_{L^2/N_h} \leq& C\Big(h^{2k}(\|\mathbf{u}_t\|^2_{k-1}+\|p\|_k^2)+\mu\|\nabla\mathbf{e}\|^2+\rho\|\nabla\cdot\mathbf{e}\|^2+\|\mathbf{u}\|_3^2\|\mathbf{e}\|^2\\ &+\big(\int_0^t \beta(t-s)\|\nabla\mathbf{e}(s)\|ds\big)^2\Big).\end{aligned}$$

We multiply both sides by $e^{2\alpha t}$ and integrate with respect to time from 0 to t. Then, the resulting double integration term can be written as a single integration similar to (3.26) and we finally reach at

$$\begin{aligned}&\int_0^t e^{2\alpha s}\|(p-p_h)(s)\|^2_{L^2/N_h}ds\\ &\leq C\Big(h^{2k}\int_0^t e^{2\alpha s}(\|\mathbf{u}_s(s)\|^2_{k-1}+\|p(s)\|_k^2)ds+\beta_1\int_0^t e^{2\alpha s}\|\nabla\mathbf{e}(s)\|^2ds\\ &\quad+\rho\int_0^t e^{2\alpha s}\|\nabla\cdot\mathbf{e}(s)\|^2ds+\|\mathbf{e}(t)\|^2_{L^\infty}\int_0^t e^{2\alpha s}\|\mathbf{u}(s)\|_3^2ds\Big).\end{aligned}$$

We use Theorem 3.1 and multiply both sides by $e^{-2\alpha t}$ to complete the rest of the proof. □

3.2. Semidiscrete error estimate for $\mathbf{H}^2$-smooth data

As discussed in the introduction, the assumption of $\mathbf{H}^m$-smooth initial data is unrealistic. So we restrict the initial velocity $\mathbf{u}_0$ to be $\mathbf{H}^2$-smooth, that is, $\mathbf{u}_0\in\mathbf{J}_1\cap\mathbf{H}^2$. The analysis of this section takes into account the lack of regularity at $t=0$.

Theorem 3.3. *Assume that* (**A1**), (**A2**), (**A3′**), (**B1**) *and* (**B2**) *hold. Let* $\alpha>0$ *be such that* $\mu-\big(\frac{\gamma}{\delta-\alpha}\big)^2>0$. *Then, there exists a positive constant* C *as defined on Theorem 3.1, such that the following bounds hold for* $t\in[0,T], T>0$ *and* $k\in\{1,2\}$

$$\|\mathbf{e}(t)\|^2+\beta_1 e^{-2\alpha t}\int_0^t e^{2\alpha s}\|\nabla\mathbf{e}(s)\|^2ds+\rho e^{-2\alpha t}\int_0^t e^{2\alpha s}\|\nabla\cdot\mathbf{e}(s)\|^2ds\leq Ch^{2k}e^{L(t)},$$

and

$$e^{-2\alpha t}\int_0^t e^{2\alpha s}\|(p-p_h)(s)\|^2_{L^2/N_h}ds\leq Ch^{2k}e^{L(t)},\quad k\in\{1,2\},$$

where, β_1, *and* $L(t)$ *are defined on Theorem 3.1.*

We skip the proof since it follows the proofs of Theorems 3.1 and 3.2.

Remark 3.4. Unlike in the case of $\mathbf{H}^m$-smooth data, where the estimates of Theorems 3.1 and 3.2 are valid for all $k \geq 1$, here, in the case of $\mathbf{H}^2$-smooth data, these estimates remain valid only for $k \in \{1, 2\}$. That is, for $k \geq 3$, for higher order approximations of velocity and pressure, we do not obtain a higher order rate of convergence but are restricted to second order convergence for velocity and pressure, in case of $\mathbf{H}^2$-smooth data, and in case the estimates do not depend on inverse power of μ.

In view of the above remark, we look into the case $k \geq 3$ for $\mathbf{H}^2$-smooth initial data. We set $\boldsymbol{\phi}_h = P_h\mathbf{e} = \mathbf{e} - (\mathbf{u} - P_h\mathbf{u})$ in (3.10) and following the steps (3.13)-(3.23), we obtain (3.24), that is,

$$\begin{aligned}
&\frac{1}{2}\frac{d}{dt}e^{2\alpha t}\|\mathbf{e}\|^2 + \frac{\mu}{2}e^{2\alpha t}\|\nabla\mathbf{e}\|^2 + \frac{\rho}{2}e^{2\alpha t}\|\nabla\cdot\mathbf{e}\|^2 + e^{2\alpha t}\int_0^t \beta(t-\tau)a(\mathbf{e}(\tau),\mathbf{e})d\tau \\
\leq&\frac{1}{2}\frac{d}{dt}e^{2\alpha t}\|\mathbf{u} - P_h\mathbf{u}\|^2 - \alpha e^{2\alpha t}\|\mathbf{u} - P_h\mathbf{u}\|^2 \\
&+ Ch^{2k}e^{2\alpha t}\left((\frac{\mu}{2} + 2\rho + 1)\|\mathbf{u}\|^2_{k+1} + \frac{2}{\rho}\|p\|^2_k\right) \\
&+ e^{2\alpha t}\Big(2\|\nabla\mathbf{u}\|_\infty + (\frac{1}{2} + \frac{2}{\rho})\|\mathbf{u}\|^2_2 + \alpha\Big)\|\mathbf{e}\|^2 \\
&+ \frac{1}{2}e^{2\alpha t}\Big(\int_0^t \beta(t-\tau)\|\nabla\mathbf{e}(\tau)\|d\tau\Big)^2. \qquad (3.36)
\end{aligned}$$

Here we can not integrate with respect to time directly since the third term on the right-hand side of (3.36) is no longer integrable near $t = 0$ for $k \geq 3$. For example, from **(A3′)**, and for $k = 3$, we have

$$\int_0^t e^{2\alpha s}\tau(s)(\|\mathbf{u}\|^2_4 + \|p\|^2_3)\; ds \leq C.$$

Here the kernel $\tau(t)$ compensates for the singularity at $t = 0$ of the higher-order estimates of the solutions.

Keeping this in mind we multiply (3.36) by $\tau^{k-2}(t)$ and use the fact $\sigma^{k-2}_t(t) \leq 2\alpha\sigma^{k-2}(t) + (k-2)\sigma^{k-3}(t)$, where $\sigma^k(t) = (\tau(t))^k e^{2\alpha t}$. Then we integrate the resulting inequality over time from 0 to t to obtain

$$\begin{aligned}
&\sigma^{k-2}(t)\|\mathbf{e}(t)\|^2 + \int_0^t \sigma^{k-2}(s)\big(\mu\|\nabla\mathbf{e}\|^2 ds + \rho\|\nabla\cdot\mathbf{e}\|^2\big)ds \\
&+ 2\int_0^t \sigma^{k-2}(s)\int_0^s \beta(s-\tau)a(\mathbf{e}(\tau),\mathbf{e}(s))d\tau ds \\
\leq\;& \sigma^{k-2}(t)\|\mathbf{u}(t) - P_h\mathbf{u}(t)\|^2 + (k-2)\int_0^t \sigma^{k-3}(s)\|\mathbf{e}(s)\|^2 ds \\
&- \int_0^t (2\alpha\sigma^{k-2}(s) + (k-2)\sigma^{k-3}(s))\|\mathbf{u}(t) - P_h\mathbf{u}(t)\|^2 ds \\
&+ Ch^{2k}\int_0^t \sigma^{k-2}(s)\left((\mu + 4\rho + 2)\|\mathbf{u}(s)\|^2_{k+1} + \frac{4}{\rho}\|p(s)\|^2_k\right)ds \\
&+ \int_0^t \sigma^{k-2}(s)\Big(2\alpha + 4\|\nabla\mathbf{u}\|_\infty + (1 + \frac{4}{\rho})\|\mathbf{u}\|^2_2\Big)\|\mathbf{e}\|^2 ds
\end{aligned}$$

$$+\int_0^t \sigma^{k-2}(s)\Big(\int_0^s \beta(s-\tau)\|\nabla \mathbf{e}(\tau)\|d\tau\Big)^2 ds. \tag{3.37}$$

However the bound for the second term on the right-hand side of (3.37), that is,

$$(k-2)\int_0^t \sigma^{k-3}(s)\|\mathbf{e}(s)\|^2 ds \tag{3.38}$$

is no longer independent of the inverse power of μ. To see this for the case $k=3$, we first split the error $\mathbf{e}$ in two parts, as $\mathbf{e} = \mathbf{u} - \mathbf{u}_h = (\mathbf{u} - \mathbf{v}_h) + (\mathbf{v}_h - \mathbf{u}_h)$, where $\mathbf{v}_h : [0,T) \to \mathbf{J}_h$ is the auxiliary function satisfying

$$(\mathbf{u}_t - \mathbf{v}_{ht}, \boldsymbol{\phi}_h) + \mu a(\mathbf{u} - \mathbf{v}_h, \boldsymbol{\phi}_h) + \int_0^t \beta(t-s) a(\mathbf{u}(\tau) - \mathbf{v}_h(\tau), \boldsymbol{\phi}_h) d\tau = 0. \tag{3.39}$$

Let $\boldsymbol{\xi} = \mathbf{u} - \mathbf{v}_h$, the choose $\boldsymbol{\phi}_h = P_h(-\Delta_h)^{-1}\boldsymbol{\xi} = (-\Delta_h)^{-1}\boldsymbol{\xi} - (-\Delta_h)^{-1}(\mathbf{u} - P_h\mathbf{u})$ in (3.39) to obtain

$$\begin{aligned}&\frac{1}{2}\frac{d}{dt}\|\boldsymbol{\xi}\|_{-1}^2 + \mu\|\boldsymbol{\xi}\|^2 + \int_0^t \beta(t-\tau)(\boldsymbol{\xi}(\tau), \boldsymbol{\xi}) d\tau \\ =&(\boldsymbol{\xi}_t, (-\Delta_h)^{-1}(\mathbf{u} - P_h\mathbf{u})) + \mu(\boldsymbol{\xi}, \mathbf{u} - P_h\mathbf{u}) + \int_0^t \beta(t-\tau)(\boldsymbol{\xi}(\tau), \mathbf{u} - P_h\mathbf{u}) d\tau.\end{aligned}$$

A use of the properties of P_h, the Cauchy-Schwarz inequality, and the Young's inequality yields

$$\begin{aligned}&\frac{d}{dt}\|\boldsymbol{\xi}\|_{-1}^2 + \mu\|\boldsymbol{\xi}\|^2 + 2\int_0^t \beta(t-\tau)(\boldsymbol{\xi}(\tau), \boldsymbol{\xi}) d\tau \\ \leq&\frac{d}{dt}\|\mathbf{u} - P_h\mathbf{u}\|_{-1}^2 + C(\mu+1)h^6\|\mathbf{u}\|_3^2 + (\int_0^t \beta(t-\tau)\|\boldsymbol{\xi}(\tau)\| d\tau)^2.\end{aligned}$$

We multiply both sides by $e^{2\alpha t}$ and integrate with respect to time to arrive at

$$\begin{aligned}&e^{2\alpha t}\|\boldsymbol{\xi}(t)\|_{-1}^2 + \mu\int_0^t e^{2\alpha s}\|\boldsymbol{\xi}(s)\|^2 ds + 2\int_0^t e^{2\alpha s}\int_0^s \beta(s-\tau)(\boldsymbol{\xi}(\tau), \boldsymbol{\xi}(s)) d\tau ds \\ \leq&2\alpha\int_0^t e^{2\alpha s}\|\boldsymbol{\xi}(s)\|_{-1}^2 ds + e^{2\alpha t}\|\mathbf{u} - P_h\mathbf{u}\|_{-1}^2 + C(\mu+1)h^6\int_0^t e^{2\alpha s}\|\mathbf{u}(s)\|_3^2 ds \\ &+ \int_0^t e^{2\alpha s}(\int_0^s \beta(s-\tau)\|\boldsymbol{\xi}(\tau)\| d\tau)^2 ds. \end{aligned} \tag{3.40}$$

We drop the double integration term on the left-hand side of (3.40) and as in (3.26) we bound the last term on the right-hand side. Now for the first term on the right-hand side, an application of the orthogonal property (3.7) of P_h and the Cauchy-Schwarz's inequality leads to

$$\begin{aligned}\|\mathbf{u} - P_h\mathbf{u}\|_{-1}^2 &= (\mathbf{u} - P_h\mathbf{u} + P_h\mathbf{u} - \mathbf{v}_h + \mathbf{v}_h - P_h\mathbf{u}, (-\Delta_h)^{-1}(\mathbf{u} - P_h\mathbf{u})) \\ &= (\boldsymbol{\xi}, (-\Delta_h)^{-1}(\mathbf{u} - P_h\mathbf{u})) \\ &\leq \|\boldsymbol{\xi}\|_{-1}\|\mathbf{u} - P_h\mathbf{u}\|_{-1}.\end{aligned}$$

Above we have used the fact that $\boldsymbol{\xi} = \mathbf{u} - \mathbf{v}_h$. On simplifying, we find

$$\|\mathbf{u} - P_h\mathbf{u}\|_{-1} \leq \|\boldsymbol{\xi}\|_{-1}. \tag{3.41}$$

Finally, a use of the Gronwall's lemma and (3.41) in (3.40) give

$$\Big(\mu - \frac{\gamma^2}{(\delta-\alpha)^2}\Big)\int_0^t e^{2\alpha s}\|\boldsymbol{\xi}(s)\|^2 ds \le Ce^{2\alpha t}(\mu+1)h^6\int_0^t e^{2\alpha s}\|\mathbf{u}(s)\|_3^2 ds.$$

We recall from Theorem 3.1 that $\beta_1 = \mu - \frac{\gamma^2}{(\delta-\alpha)^2} > 0$. Now the resulting estimate will depend on the inverse power of μ. Using similar arguments we can show that the estimate of (3.38) will depend on the inverse power of μ for $k > 3$. As a result, so will the estimate of (3.37).

In order to show that only second-order convergence is possible, in case estimates are independent of inverse power of μ, and in case $k \ge 3$, we obtain (3.36) as earlier. But now we restrict ourselves to lower order projection properties, that is, $\|\nabla(\mathbf{u} - P_h\mathbf{u})\| \le Ch^2\|\mathbf{u}\|_3$, etc., which no longer demands a time weight $\tau(t)$. Following the lines of argument for (3.24), we can obtain the desired result.

4. Backward Euler method

In this section, we consider the full discretization of the finite element approximation (3.3). We apply a backward Euler method for time discretization. Let $\{t_n\}_{n=0}^N$ be a uniform partition of the time interval $[0,T]$ and $t_n = n\Delta t$ with time step $\Delta t > 0$. We approximate the time derivative term of the Oldroyd model of order one by

$$\partial_t\phi^n = \frac{(\phi^n - \phi^{n-1})}{\Delta t},$$

where $\phi^n = \phi(t_n)$ a sequence in $\mathbf{H}_h$ which is defined on $[0,T]$. Since the backward Euler method is of the first order in time, so for the integration term, we apply the right rectangle rule as

$$q_r^n(\boldsymbol{\phi}) = \Delta t\sum_{j=0}^n \beta(t_n - t_j)\boldsymbol{\phi}^j \approx \int_0^t \beta(t_n - s)\boldsymbol{\phi}(s)ds.$$

It is observed that the right rectangle rule [41] is positive in the sense that

$$\Delta t\sum_{i=1}^n q_r^i(\boldsymbol{\phi}) = \Delta t\sum_{i=1}^n \Big(\Delta t\sum_{j=0}^i \beta(t_n - t_j)\boldsymbol{\phi}^j\Big)\boldsymbol{\phi}^i \ge 0. \tag{4.1}$$

Now the backward Euler method applied in (3.3) is stated as below: Find $\mathbf{U}^n \in \mathbf{H}_h$ and $P^n \in L_h$ such that for $\mathbf{U}(0) = P_h\mathbf{u}_0$ and $t > 0$

$$\left.\begin{aligned} &(\partial_t\mathbf{U}^n, \boldsymbol{\phi}_h) + \mu a(\mathbf{U}^n, \boldsymbol{\phi}_h) + b(\mathbf{U}^n, \mathbf{U}^n, \boldsymbol{\phi}_h) \\ &\quad -(P^n, \nabla\cdot\boldsymbol{\phi}_h) + \rho(\nabla\cdot\mathbf{U}^n, \nabla\cdot\boldsymbol{\phi}_h) \\ &= (\mathbf{f}^n, \boldsymbol{\phi}_h) - a(q_r^n(\mathbf{U}), \boldsymbol{\phi}_h), \quad \forall\ \boldsymbol{\phi}_h \in \mathbf{H}_h, \\ &(\nabla\cdot\mathbf{U}^n, \chi_h) = 0, \quad \forall\ \chi_h \in L_h. \end{aligned}\right\} \tag{4.2}$$

If we consider the discrete solution $\mathbf{U}^n \in \mathbf{J}_h$, then (4.2) becomes: Find $\mathbf{U}^n \in \mathbf{J}_h$ such that for $\mathbf{U}(0) = P_h\mathbf{u}_0$ and $t > 0$

$$(\partial_t\mathbf{U}^n, \boldsymbol{\phi}_h) + \mu a(\mathbf{U}^n, \boldsymbol{\phi}_h) + b(\mathbf{U}^n, \mathbf{U}^n, \boldsymbol{\phi}_h) + \rho(\nabla\cdot\mathbf{U}^n, \nabla\cdot\boldsymbol{\phi}_h)$$

$$=(\mathbf{f}^n, \boldsymbol{\phi}_h) - a(q_r^n(\mathbf{U}), \boldsymbol{\phi}_h), \quad \forall\ \boldsymbol{\phi}_h \in \mathbf{J}_h. \tag{4.3}$$

Using a variant of Brouwer fixed point theorem and standard uniqueness arguments, it is easy to show that the discrete problem (4.2) or (4.3) is well-posed. We can prove *a priori* bounds for the fully discrete solution $\{\mathbf{U}^n\}_{1\le n\le N}$ similar to Lemma 3.1, which helps us to prove the local existence of the fully discrete solution (for a similar proof, see [6]).

4.1. Fully discrete error estimates for $\mathbf{H}^m$-smooth data

We define $\mathbf{u}(t_n) = \mathbf{u}^n$, $p(t_n) = p^n$ and set $\mathbf{e}^n = \mathbf{U}^n - \mathbf{u}^n$. For the error equation, we consider (3.9) at $t = t_n$ and subtract the resulting equation from (4.3): For all $\boldsymbol{\phi}_h \in \mathbf{J}_h$

$$\begin{aligned}
&(\partial_t \mathbf{e}^n, \boldsymbol{\phi}_h) + \mu a(\mathbf{e}^n, \boldsymbol{\phi}_h) + \rho(\nabla\cdot\mathbf{e}^n, \nabla\cdot\boldsymbol{\phi}_h) + a(q_r^n(\mathbf{e}), \boldsymbol{\phi}_h) \\
=&(p^n, \nabla\cdot\boldsymbol{\phi}_h) + R^n(\boldsymbol{\phi}_h) + \Lambda^n(\boldsymbol{\phi}_h) + E^n(\boldsymbol{\phi}_h),
\end{aligned} \tag{4.4}$$

where

$$\begin{aligned}
R^n(\boldsymbol{\phi}_h) &= (\mathbf{u}_t^n, \boldsymbol{\phi}_h) - (\partial_t \mathbf{u}^n, \boldsymbol{\phi}_h) \\
&= (\mathbf{u}_t^n, \boldsymbol{\phi}_h) - \frac{1}{\Delta t}\int_{t_{n-1}}^{t_n} (\mathbf{u}_s, \boldsymbol{\phi}_h)\ ds \\
&= \frac{1}{\Delta t}\int_{t_{n-1}}^{t_n} (s - t_{n-1})(\mathbf{u}_{ss}, \boldsymbol{\phi}_h)\ ds,
\end{aligned} \tag{4.5}$$

$$E^n(\boldsymbol{\phi}_h) = \int_0^{t_n} \beta(t-s)a(\mathbf{u}(s), \boldsymbol{\phi}_h)\ ds - \Delta t\sum_{i=1}^n \beta(t_n - t_i)a(\mathbf{u}^i, \boldsymbol{\phi}_h) \tag{4.6}$$

$$\le C\sum_{i=1}^n \int_{t_{i-1}}^{t_i} (s - t_{i-1})\big(\beta_s(t_n - s)a(\mathbf{u}(s), \boldsymbol{\phi}_h) + \beta(t_n - s)a(\mathbf{u}_s(s), \boldsymbol{\phi}_h)\big)\ ds,$$

$$\begin{aligned}
\Lambda^n(\boldsymbol{\phi}_h) &= b(\mathbf{u}^n, \mathbf{u}^n, \boldsymbol{\phi}_h) - b(\mathbf{U}^n, \mathbf{U}^n, \boldsymbol{\phi}_h) \\
&= b(\mathbf{e}^n, \mathbf{e}^n, \boldsymbol{\phi}_h) - b(\mathbf{u}^n, \mathbf{e}^n, \boldsymbol{\phi}_h) - b(\mathbf{e}^n, \mathbf{u}^n, \boldsymbol{\phi}_h).
\end{aligned} \tag{4.7}$$

4.1.1. Fully discrete error bounds for velocity

In this section, we consider the exact solution to be $\mathbf{H}^m$-smooth. Our main result of this section is as follows:

Theorem 4.1. *Let the initial velocity satisfy $\mathbf{u}_0 \in \mathbf{H}^{\max\{3,k\}}$ and let all other assumptions of Theorem 3.1 hold true. Further, let $\mathbf{u}_t \in L^2(0,T;\mathbf{H}^2)\cap L^2(0,T;\mathbf{H}^k)$ and $\mathbf{u}_{tt} \in L^2(0,T;\mathbf{L}^2)$. Then there exists a positive constant C, independent of the inverse power of μ, such that the following bounds hold for $1 \le n \le N$*

$$\begin{aligned}
&\|\mathbf{e}^n\|^2 + \beta_1 \Delta t e^{-2\alpha t_n}\sum_{i=1}^n e^{2\alpha t_i}\|\nabla\mathbf{e}^i\|^2 + \rho\Delta t e^{-2\alpha t_n}\sum_{i=1}^n e^{2\alpha t_i}\|\nabla\cdot\mathbf{e}^i\|^2 \\
\le& Ce^{\hat{L}^n}\big(K_1(t_n)h^{2k} + K_2(t_n)(\Delta t)^2\big),
\end{aligned}$$

where $\beta_1 = \mu - \big(\frac{\gamma}{\delta-\alpha}\big)^2 > 0$, and

$$\hat{L}^n = \sum_{i=1}^n \big(C(\alpha) + 4\|\nabla\mathbf{u}^i\|_\infty + (1 + \frac{4}{\rho})\|\mathbf{u}^i\|_2^2\big), \tag{4.8}$$

$$
\begin{aligned}
K_1(t_n) &= e^{-2\alpha t_n}\int_0^{t_n} e^{2\alpha s}\big(\|\mathbf{u}_s(s)\|_k^2+(\mu+4\rho+2)\|\mathbf{u}(s)\|_{k+1}^2+\frac{4}{\rho}\|p(s)\|_k^2\big)ds\\
&\quad+\|\mathbf{u}(t_n)\|_k^2,\\
K_2(t_n) &= e^{-2\alpha t_n}\int_0^{t_n} e^{2\alpha s}\big(\|\mathbf{u}_{ss}(s)\|^2+\|\mathbf{u}(s)\|_2^2+\|\mathbf{u}_s(s)\|_2^2\big)ds.
\end{aligned}
$$

Proof. We take $n=i$ and $\boldsymbol{\phi}_h = P_h\mathbf{e}^i = \mathbf{e}^i - (\mathbf{u}^i - P_h\mathbf{u}^i)$ in (4.4) to arrive at

$$
\begin{aligned}
&(\partial_t\mathbf{e}^i,\mathbf{e}^i)+\mu a(\mathbf{e}^i,\mathbf{e}^i)+\rho(\nabla\cdot\mathbf{e}^i,\nabla\cdot\mathbf{e}^i)+a(q_r^i(\mathbf{e}),\mathbf{e}^i)\\
=&(\partial_t\mathbf{e}^i,\mathbf{u}^i-P_h\mathbf{u}^i)+\mu a(\mathbf{e}^i,\mathbf{u}^i-P_h\mathbf{u}^i)+\rho(\nabla\cdot\mathbf{e}^i,\nabla\cdot(\mathbf{u}^i-P_h\mathbf{u}^i))\\
&+a(q_r^i(\mathbf{e}),\mathbf{u}^i-P_h\mathbf{u}^i)+(p^n,\nabla\cdot P_h\mathbf{e}^i)+R_h^i(P_h\mathbf{e}^i)+\Lambda_h^i(P_h\mathbf{e}^i)+E_h^i(P_h\mathbf{e}^i).
\end{aligned}
$$

We note that

$$
(\partial_t\boldsymbol{\phi}^i,\boldsymbol{\phi}^i)=\frac{1}{\Delta t}(\boldsymbol{\phi}^i-\boldsymbol{\phi}^{i-1},\boldsymbol{\phi}^i)=\frac{1}{2}\partial_t\|\boldsymbol{\phi}^i\|^2+\frac{\Delta t}{2}\|\partial_t\boldsymbol{\phi}^i\|^2\geq\frac{1}{2}\partial_t\|\boldsymbol{\phi}^i\|^2. \tag{4.9}
$$

A use of the approximation property (3.7) of P_h yields

$$
\begin{aligned}
(\partial_t\mathbf{e}^i,\mathbf{u}^i-P_h\mathbf{u}^i)&=(\partial_t(\mathbf{u}^i-P_h\mathbf{u}^i),\mathbf{u}^i-P_h\mathbf{u}^i)\\
&\leq Ch^{2k}(\frac{1}{2}\partial_t\|\mathbf{u}^i\|_k^2+\frac{\Delta t}{2}\|\partial_t\mathbf{u}^i\|_k^2).
\end{aligned} \tag{4.10}
$$

We now apply the Cauchy-Schwarz inequality and the Young's inequality along with (3.7), (4.9) and (4.10) to obtain

$$
\begin{aligned}
&\partial_t\|\mathbf{e}^i\|^2+\mu\|\nabla\mathbf{e}^i\|^2+\frac{3\rho}{2}\|\nabla\cdot\mathbf{e}^i\|^2+2a(q_r^i(\mathbf{e}),\mathbf{e}^i)\\
\leq& Ch^{2k}\Big(\partial_t\|\mathbf{u}^i\|_k^2+\Delta t\|\partial_t\mathbf{u}^i\|_k^2+(\mu+4\rho+1)\|\mathbf{u}^i\|_{k+1}^2+\frac{4}{\rho}\|p^i\|_k^2\Big)\\
&+(q_r^i(\|\nabla\mathbf{e}\|))^2+2R_h^i(P_h\mathbf{e}^i)+2\Lambda_h^i(P_h\mathbf{e}^i)+2E_h^i(P_h\mathbf{e}^i).
\end{aligned}
$$

We multiply both side by $\Delta t e^{2\alpha t_i}$ then sum over $i=1$ to n to find that,

$$
\begin{aligned}
&\Delta t\sum_{i=1}^n e^{2\alpha t_i}\partial_t\|\mathbf{e}^i\|^2+\mu\Delta t\sum_{i=1}^n e^{2\alpha t_i}\|\nabla\mathbf{e}^i\|^2\\
&+\frac{3\rho}{2}\Delta t\sum_{i=1}^n e^{2\alpha t_i}\|\nabla\cdot\mathbf{e}^i\|^2+2\Delta t\sum_{i=1}^n e^{2\alpha t_i}a(q_r^i(\mathbf{e}),\mathbf{e}^i)\\
\leq& Ch^{2k}\Delta t\sum_{i=1}^n e^{2\alpha t_i}\Big(\partial_t\|\mathbf{u}^i\|_k^2+\Delta t\|\partial_t\mathbf{u}^i\|_k^2+(\mu+4\rho+1)\|\mathbf{u}^i\|_{k+1}^2+\frac{4}{\rho}\|p^i\|_k^2\Big)\\
&+\Delta t\sum_{i=1}^n e^{2\alpha t_i}(q_r^i(\|\nabla\mathbf{e}\|))^2+2\Delta t\sum_{i=1}^n e^{2\alpha t_i}(R^i(P_h\mathbf{e}^i)+\Lambda^i(P_h\mathbf{e}^i)+E^i(P_h\mathbf{e}^i)).
\end{aligned} \tag{4.11}
$$

The positivity property (4.1) gives us

$$
\Delta t\sum_{i=1}^n e^{2\alpha t_i}a(q_r^i(\mathbf{e}),\mathbf{e}^i)=\Delta t\sum_{i=1}^n e^{2\alpha t_i}\Delta t\sum_{j=1}^i\beta(t_i-t_j)\|\nabla\mathbf{e}^j\|\|\nabla\mathbf{e}^i\|\geq 0. \tag{4.12}
$$

Similar to (3.26), with a use of Cauchy-Schwarz inequality and the change of order of summation, we can write the second term on the right-hand side of (4.11) as

$$\begin{aligned}\Delta t\sum_{i=1}^{n} e^{2\alpha t_i}(q_r^i(\|\nabla \mathbf{e}\|))^2 &= \Delta t\sum_{i=1}^{n} e^{2\alpha t_i}\Delta t\sum_{j=0}^{i}\beta(t_n-t_j)\|\nabla \mathbf{e}^j\|^2\\ &\le \Big(\frac{\gamma}{\delta-\alpha}\Big)^2\Delta t\sum_{i=1}^{n} e^{2\alpha t_i}\|\nabla \mathbf{e}^i\|^2. \end{aligned}\tag{4.13}$$

Now use the fact that

$$\begin{aligned}\Delta t\sum_{i=1}^{n} e^{2\alpha t_i}\partial_t\|\mathbf{e}^i\|^2 &= \sum_{i=1}^{n} e^{2\alpha t_i}(\|\mathbf{e}^i\|^2-\|\mathbf{e}^{i-1}\|^2)\\ &= e^{2\alpha t_n}\|\mathbf{e}^n\|^2-\sum_{i=1}^{n-1} e^{2\alpha t_i}(e^{2\alpha\Delta t}-1)\|\mathbf{e}^i\|^2\end{aligned}$$

in (4.11) and then use (4.12) and (4.13) with $\beta_1=\mu-(\frac{\gamma}{\delta-\alpha})^2>0$ to arrive at

$$\begin{aligned}&e^{2\alpha t_n}\|\mathbf{e}^n\|^2+\beta_1\Delta t\sum_{i=1}^{n} e^{2\alpha t_i}\|\nabla\mathbf{e}^i\|^2+\frac{3\rho}{2}\Delta t\sum_{i=1}^{n} e^{2\alpha t_i}\|\nabla\cdot\mathbf{e}^i\|^2\\ &\le\sum_{i=1}^{n-1} e^{2\alpha t_i}(e^{2\alpha\Delta t}-1)\|\mathbf{e}^i\|^2+Ch^{2k}\Big[e^{2\alpha t_n}\|\mathbf{u}^n\|_k^2-\|\mathbf{u}_0\|^2\\ &\quad-\sum_{i=1}^{n-1} e^{2\alpha t_i}(e^{2\alpha\Delta t}-1)\|\mathbf{u}^i\|^2+(\Delta t)^2\sum_{i=1}^{n} e^{2\alpha t_i}\|\partial_t\mathbf{u}^i\|_k^2\\ &\quad+\Delta t\sum_{i=1}^{n} e^{2\alpha t_i}\Big((\mu+4\rho+1)\|\mathbf{u}^i\|_{k+1}^2+\frac{4}{\rho}\|p^i\|_k^2\Big)\Big]\\ &\quad+2\Delta t\sum_{i=1}^{n} e^{2\alpha t_i}(R^i(P_h\mathbf{e}^i)+\Lambda^i(P_h\mathbf{e}^i)+E^i(P_h\mathbf{e}^i)).\end{aligned}\tag{4.14}$$

The second and third terms within the bracket on the right-hand side are positive, so we drop them and the third and fourth terms can be written as

$$\begin{aligned}(\Delta t)^2\sum_{i=1}^{n} e^{2\alpha t_i}\|\partial_t\mathbf{u}^i\|_k^2 &\le (\Delta t)^2\sum_{i=1}^{n} e^{2\alpha t_i}\Big(\frac{1}{\Delta t}\int_{t_{i-1}}^{t_i}\|\mathbf{u}_s(s)\|_k ds\Big)^2\\ &\le C\int_0^{t_n} e^{2\alpha s}\|\mathbf{u}_s(s)\|_k^2 ds,\end{aligned}\tag{4.15}$$

and

$$\begin{aligned}&\Delta t\sum_{i=1}^{n} e^{2\alpha t_i}\Big((\mu+4\rho+1)\|\mathbf{u}^i\|_{k+1}^2+\frac{4}{\rho}\|p^i\|_k^2\Big)\\ &\le\int_0^{t_n} e^{2\alpha s}\Big((\mu+4\rho+1)\|\mathbf{u}(s)\|_{k+1}^2+\frac{4}{\rho}\|p(s)\|_k^2\Big)ds.\end{aligned}\tag{4.16}$$

A use of the Cauchy-Schwarz inequality and the Young's inequality with $t_{i-1} \leq t,\ t \in [t_{i-1}, t_i]$ in (4.5) yields

$$
\begin{aligned}
&\Delta t \sum_{i=1}^{n} e^{2\alpha t_i} R^i(P_h \mathbf{e}^i) \\
\leq& \Delta t \sum_{i=1}^{n} e^{2\alpha t_i} \frac{1}{\Delta t} \int_{t_{i-1}}^{t_i} (s - t_{i-1}) \|\mathbf{u}_{ss}(s)\| ds \ \|P_h \mathbf{e}^i\| \\
\leq& \Delta t \sum_{i=1}^{n} e^{2\alpha t_i} \Big(\frac{1}{\Delta t} \int_{t_{i-1}}^{t_i} (s - t_{i-1}) \|\mathbf{u}_{ss}(s)\| ds \Big)^2 + \frac{1}{4} \Delta t \sum_{i=1}^{n} e^{2\alpha t_i} \|\mathbf{e}^i\|^2 \\
\leq& \Delta t \sum_{i=1}^{n} e^{2\alpha t_i} \frac{1}{(\Delta t)^2} \Big(\int_{t_{i-1}}^{t_i} (s - t_{i-1})^2 ds \Big) \Big(\int_{t_{i-1}}^{t_i} \|\mathbf{u}_{ss}(s)\|^2 ds \Big) \\
&+ \frac{\Delta t}{4} \sum_{i=1}^{n} e^{2\alpha t_i} \|\mathbf{e}^i\|^2 \\
\leq& (\Delta t)^2 \sum_{i=1}^{n} e^{2\alpha t_i} \int_{t_{i-1}}^{t_i} \|\mathbf{u}_{ss}(s)\|^2 ds + \frac{\Delta t}{4} \sum_{i=1}^{n} e^{2\alpha t_i} \|\mathbf{e}^i\|^2 \\
\leq& C e^{2\alpha \Delta t} (\Delta t)^2 \int_0^{t_n} e^{2\alpha s} \|\mathbf{u}_{ss}(s)\|^2 ds + \frac{1}{4} \Delta t \sum_{i=1}^{n} e^{2\alpha t_i} \|\mathbf{e}^i\|^2. \qquad (4.17)
\end{aligned}
$$

Again, an application of the Cauchy-Schwarz inequality and the Young's inequality in (4.6) give

$$
\begin{aligned}
&\Delta t \sum_{i=1}^{n} e^{2\alpha t_i} |E^i(P_h \mathbf{e}^i)| \\
\leq& C \Delta t \sum_{i=1}^{n} e^{2\alpha t_i} \Big(\sum_{j=1}^{i} \int_{t_{j-1}}^{t_j} (s - t_{j-1}) \beta(t_i - s) \big| \delta \|\tilde{\Delta} \mathbf{u}(s)\| + \|\tilde{\Delta} \mathbf{u}_s(s)\|) \big| ds \Big) \|P_h \mathbf{e}^i\| \\
\leq& C \Delta t \sum_{i=1}^{n} e^{2\alpha t_i} \Big(\sum_{j=1}^{i} \int_{t_{j-1}}^{t_j} (s - t_{j-1}) \beta(t_i - s) \big(\delta \|\mathbf{u}(s)\|_2 + \|\mathbf{u}_s(s)\|_2 \big) ds \Big)^2 \\
&+ \frac{1}{4} \Delta t \sum_{i=1}^{n} e^{2\alpha t_i} \|\mathbf{e}^i\|^2 \\
\leq& C (\Delta t)^2 \int_0^{t_n} e^{2\alpha s} (\|\mathbf{u}(s)\|_2^2 + \|\mathbf{u}_s(s)\|_2^2) ds + \frac{1}{4} \Delta t \sum_{i=1}^{n} e^{2\alpha t_i} \|\mathbf{e}^i\|^2. \qquad (4.18)
\end{aligned}
$$

Also, similar to (3.19)-(3.23), we can bound the nonlinear terms of (4.7) as

$$
\begin{aligned}
|\Lambda^i(P_h \mathbf{e}^i)| \leq& |b(\mathbf{u}^i, \mathbf{e}^i, \mathbf{u}^i - P_h \mathbf{u}^i)| + |b(\mathbf{e}^i, \mathbf{u}^i, \mathbf{e}^i)| \\
&+ |b(\mathbf{e}^i, \mathbf{u}^i, \mathbf{u}^i - P_h \mathbf{u}^i)| + |b(\mathbf{e}^i, \mathbf{e}^i, \mathbf{u}^i - P_h \mathbf{u}^i)| \\
\leq& C h^{2k} \|\mathbf{u}^i\|_{k+1}^2 + (2\|\nabla \mathbf{u}^i\|_\infty + (\frac{1}{2} + \frac{2}{\rho}) \|\mathbf{u}^i\|_2^2) \|\mathbf{e}^i\|^2 + \frac{\rho}{4} \|\nabla \cdot \mathbf{e}^i\|^2.
\end{aligned}
$$

Hence,

$$
\Delta t \sum_{i=1}^{n} e^{2\alpha t_i} |\Lambda^i(P_h \mathbf{e}^i)| \leq C h^{2k} \Delta t \sum_{i=1}^{n} e^{2\alpha t_i} \|\mathbf{u}^i\|_{k+1}^2 + \frac{\rho}{4} \Delta t \sum_{i=1}^{n} e^{2\alpha t_i} \|\nabla \cdot \mathbf{e}^i\|^2
$$

$$+ C\Delta t\sum_{i=1}^{n} e^{2\alpha t_i}(2\|\nabla \mathbf{u}^i\|_\infty + (1+\frac{1}{2\rho})\|\mathbf{u}^i\|_2^2)\|\mathbf{e}^i\|^2. \quad (4.19)$$

Now, we use (4.15)-(4.19) in (4.14) to arrive at

$$\begin{aligned}
&e^{2\alpha t_n}\|\mathbf{e}^n\|^2 + \beta_1\Delta t\sum_{i=1}^{n} e^{2\alpha t_i}\|\nabla\mathbf{e}^i\|^2 + \rho\Delta t\sum_{i=1}^{n} e^{2\alpha t_i}\|\nabla\cdot\mathbf{e}^i\|^2 \\
\le& Ch^{2k}\Big[\int_0^{t_n} e^{2\alpha s}\big(\|\mathbf{u}_s(s)\|_k^2 + (\mu+4\rho+2)\|\mathbf{u}(s)\|_{k+1}^2 + \frac{4}{\rho}\|p(s)\|_k^2\big)ds\Big] \\
&+ Ch^{2k}e^{2\alpha t_n}\|\mathbf{u}(t_n)\|_k^2 + C(\Delta t)^2\int_0^{t_n} e^{2\alpha s}\big(\|\mathbf{u}_{ss}\|^2 + \|\mathbf{u}(s)\|_2^2 + \|\mathbf{u}_s(s)\|_2^2\big)ds \\
&+ \Delta t\sum_{i=1}^{n} e^{2\alpha t_i}\big(\frac{e^{2\alpha\Delta t}-1}{\Delta t} + 4\|\nabla\mathbf{u}^i\|_\infty + (1+\frac{4}{\rho})\|\mathbf{u}^i\|_2^2\big)\|\mathbf{e}^i\|^2.
\end{aligned}$$

Note that $e^{2\alpha\Delta t} - 1 \le C(\alpha)\Delta t$. We now apply the discrete Gronwall's Lemma and then multiply the resulting equation by $e^{-2\alpha t_n}$ to complete the rest of the proof. □

Remark 4.1. From (**A3**), $\hat{L}^n$ defined in (4.8) is bounded by Ct_n and $K_1(t_n)$ and $K_2(t_n)$ defined in (3.12) and (3.27) respectively, both are bounded by C, where C is not dependent of inverse power of μ.

4.1.2. Fully discrete error bounds for pressure

To obtain the fully discrete pressure error estimate, first, we consider (3.9) with $t = t_n$ and subtract (4.2) from the resulting equation to arrive at

$$\begin{aligned}
(p^n - P^n, \nabla\cdot\boldsymbol{\phi}_h) =& (\partial_t\mathbf{e}^n, \boldsymbol{\phi}_h) + \mu a(\mathbf{e}^n, \boldsymbol{\phi}_h) + \rho(\nabla\cdot\mathbf{e}^n, \nabla\cdot\boldsymbol{\phi}_h) + a(q_r^n(\mathbf{e}), \boldsymbol{\phi}_h) \\
&+ R^n(\boldsymbol{\phi}_h) + \Lambda^n(\boldsymbol{\phi}_h) + E^n(\boldsymbol{\phi}_h).
\end{aligned}$$

A use of (4.5), (4.6), (4.7) with the Cauchy-Schwarz inequality yields

$$\begin{aligned}
&(p^n - P^n, \nabla\cdot\boldsymbol{\phi}_h) \\
\le& C\Bigg[\|\partial_t\mathbf{e}^n\|_{-1} + \mu\|\nabla\mathbf{e}^n\| + \rho\|\nabla\cdot\mathbf{e}^n\| + \|q_r^n(\nabla\mathbf{e})\| \\
&+ \sum_{i=1}^{n}\int_{t_{i-1}}^{t_i}(s-t_{i-1})\big(\beta_s(t_n-s)\|\nabla\mathbf{u}(s)\| + \beta(t_n-s)\|\nabla\mathbf{u}_s(s)\|\big)\,ds \\
&+ \frac{1}{\Delta t}\int_{t_{n-1}}^{t_n}(s-t_{n-1})\|\mathbf{u}_{ss}(s)\|_{-1}\,ds + (\|\mathbf{u}^n\|_2 + \|\mathbf{U}^n\|_2)\|\mathbf{e}^n\|\Bigg]\|\nabla\boldsymbol{\phi}_h\|. \quad (4.20)
\end{aligned}$$

Arguing as in the proof of Lemma 3.2, we can bound the first term on the right-hand side of (4.20) as

$$\begin{aligned}
\|\partial_t\mathbf{e}^n\|_{-1} \le& C\Bigg[h^{2k}\|\partial_t\mathbf{u}^n\|_{k-1} + \mu\|\nabla\mathbf{e}^n\| + \rho\|\nabla\cdot\mathbf{e}^n\| + \|q_r^n(\nabla\mathbf{e})\| \\
&+ \sum_{i=1}^{n}\int_{t_{i-1}}^{t_i}(s-t_{i-1})\big(\beta_s(t_n-s)\|\nabla\mathbf{u}(s)\| + \beta(t_n-s)\|\nabla\mathbf{u}_s(s)\|\big)\,ds
\end{aligned}$$

$$+\frac{1}{\Delta t}\int_{t_{n-1}}^{t_n}(s-t_{n-1})\|\mathbf{u}_{ss}(s)\|_{-1}\ ds+(\|\mathbf{u}^n\|_2+\|\mathbf{U}^n\|_2)\|\mathbf{e}^n\|\Big]. \quad (4.21)$$

Incorporate (4.21) in (4.20) and divide the resulting inequality by $\|\nabla\boldsymbol{\phi}_h\|,\ \boldsymbol{\phi}_h\neq 0$. Similar to (3.29), we then have

$$\begin{aligned}&\|p^n-P^n\|_{L^2/N_h}\\ \leq& C\Big[h^k(\|\partial_t\mathbf{u}^n\|_{k-1}+\|p^n\|_k)+\mu\|\nabla\mathbf{e}^n\|+\rho\|\nabla\cdot\mathbf{e}^n\|+\|q_r^n(\nabla\mathbf{e})\|\\ &+\frac{1}{\Delta t}\int_{t_{n-1}}^{t_n}(s-t_{n-1})\|\mathbf{u}_{ss}(s)\|_{-1}\ ds+(\|\mathbf{u}^n\|_2+\|\mathbf{U}^n\|_2)\|\mathbf{e}^n\|\\ &+\sum_{i=1}^n\int_{t_{i-1}}^{t_i}(s-t_{i-1})\big(\beta_s(t_n-s)\|\nabla\mathbf{u}(s)\|+\beta(t_n-s)\|\nabla\mathbf{u}_s(s)\|\big)ds\Big].\end{aligned}$$

Squaring and multiplying both side by $\Delta te^{2\alpha t_n}$ with $n=i$ and taking sum from $i=1$ to n to obtain

$$\begin{aligned}&\Delta t\sum_{i=1}^n\|p^i-P^i\|^2_{L^2/N_h}\\ \leq& C\Delta t\sum_{i=1}^n\Big[h^{2k}(\|\partial_t\mathbf{u}^i\|^2_{k-1}+\|p^i\|^2_k)+\mu\|\nabla\mathbf{e}^i\|^2+\rho\|\nabla\cdot\mathbf{e}^i\|^2\\ &+\|q_r^i(\nabla\mathbf{e})\|^2+\Big(\frac{1}{\Delta t}\int_{t_{i-1}}^{t_i}(s-t_{i-1})\|\mathbf{u}_{ss}(s)\|_{-1}\ ds\Big)^2+(\|\mathbf{u}^i\|^2_2+\|\mathbf{U}^i\|^2_2)\|\mathbf{e}^i\|^2\\ &+\Big(\sum_{j=1}^i\int_{t_{j-1}}^{t_j}(s-t_{j-1})\big(\beta_s(t_i-s)\|\nabla\mathbf{u}(s)\|+\beta(t_i-s)\|\nabla\mathbf{u}_s(s)\|\big)\ ds\Big)^2\Big].\end{aligned}$$

A use of Theorem 4.1 and the Young's inequality leads to

$$\begin{aligned}&\Delta t\sum_{i=1}^n\|p^i-P^i\|^2_{L^2/N_h}\\ \leq& Ce^{\hat{L}t_n}h^{2k}\Big(\|\mathbf{u}(t_n)\|^2_k\\ &+e^{-2\alpha t_n}\int_0^{t_n}e^{2\alpha s}\big(\|\mathbf{u}_s(s)\|^2_k+(\mu+4\rho+2)\|\mathbf{u}(s)\|^2_{k+1}+\frac{4}{\rho}\|p(s)\|^2_k\big)ds\Big)\\ &+Ce^{\hat{L}t_n}(\Delta t)^2e^{-2\alpha t_n}\int_0^{t_n}e^{2\alpha s}\big(\|\mathbf{u}_{ss}(s)\|^2+\|\mathbf{u}(s)\|^2_2+\|\mathbf{u}_s(s)\|^2_2\big)ds.\end{aligned}$$

Multiply both sides by $e^{-2\alpha t}$. We summarize our result in the following Theorem.

Theorem 4.2. *Under the assumption of theorem 4.1, the following holds true:*

$$\Delta te^{-2\alpha t_n}\sum_{i=0}^n e^{2\alpha t_i}\|p^n-P^n\|^2_{L^2/N_h}\leq Ce^{\hat{L}^n}\big(K_1(t_n)h^{2k}+K_2(t_n)(\Delta t)^2\big).$$

4.2. Fully discrete error estimates for $\mathbf{H}^2$-smooth data

We now consider, the initial data $\mathbf{u}_0\in\mathbf{J}_1\cap\mathbf{H}^2$. Then, the following result holds.

Theorem 4.3. *Let the assumptions of Theorem 3.3 hold true. Further, let $\tau(t)\mathbf{u}_t \in L^2(0,T;\mathbf{H}^2)$ and $\tau(t)\mathbf{u}_{tt} \in L^2(0,T;\mathbf{L}^2)$. Then there exists a positive constant C, independent of the inverse power of μ, such that the following bounds hold for $1 \leq n \leq N$ and $k \in \{1,2\}$*

$$\begin{aligned}
&\|\mathbf{e}^n\|^2 + \beta_1 \Delta t e^{-2\alpha t_n} \sum_{i=1}^{n} e^{2\alpha t_i} \|\nabla \mathbf{e}^i\|^2 + \rho \Delta t e^{-2\alpha t_n} \sum_{i=1}^{n} e^{2\alpha t_i} \|\nabla \cdot \mathbf{e}^i\|^2 \\
\leq & C e^{\hat{L}^n} \big(K_3(t_n) h^{2k} + K_4(t_n)\Delta t \big),
\end{aligned}$$

and

$$\Delta t e^{-2\alpha t_n} \sum_{i=0}^{n} e^{2\alpha t_i} \|p^n - P^n\|^2_{L^2/N_h} \leq C e^{\hat{L}^n} \big(K_3(t_n) h^{2k} + K_4(t_n)\Delta t \big),$$

where $\beta_1 = \mu - \big(\frac{\gamma}{\delta-\alpha}\big)^2 > 0$, and $\hat{L}^n$ is defined in (4.8), and

$$\begin{aligned}
K_3(t_n) = & e^{-2\alpha t_n} \int_0^{t_n} e^{2\alpha s} \tau^{k-1}(s) \big(\|\mathbf{u}_s(s)\|_k^2 + (\mu + 4\rho + 2) \|\mathbf{u}(s)\|^2_{k+1} + \frac{4}{\rho} \|p(s)\|_k^2 \big) ds \\
& + \|\mathbf{u}(t_n)\|_k^2,
\end{aligned}$$

and

$$K_4(t_n) = e^{-2\alpha t_n} \int_0^{t_n} e^{2\alpha s} \tau(s) \big(\|\mathbf{u}_{ss}(s)\|^2 + \|\mathbf{u}(s)\|_2^2 + \|\mathbf{u}_s(s)\|_2^2 \big) ds.$$

Proof. The proof goes in the similar way of the proof of Theorem 4.1 except the estimates (4.15), (4.17) and (4.18) since $\|\mathbf{u}_{tt}(t)\|$ and $\|\mathbf{u}_t(t)\|_2$ are not integrable at $t = 0$, when $\mathbf{u}_0 \in \mathbf{J}_1 \cap \mathbf{H}^2$. For $k = 1$, (4.15) will go through as it is but for $k = 2$, we modify it as follows, keeping in mind $\tau(t_n) \leq \tau(t_{n-1}) + \Delta t \leq C\tau(t)$ for $t \in [t_{n-1}, t_n]$

$$\begin{aligned}
(\Delta t)^2 \sum_{i=1}^{n} e^{2\alpha t_i} \|\partial_t \mathbf{u}^i\|_2^2 & \leq (\Delta t)^2 \sum_{i=1}^{n} e^{2\alpha t_i} \Big(\frac{1}{\Delta t} \int_{t_{i-1}}^{t_i} \|\mathbf{u}_s(s)\|_2 ds \Big)^2 \\
& \leq e^{2\alpha \Delta t} \sum_{i=1}^{n} \Big(\int_{t_{i-1}}^{t_i} \frac{1}{\tau(t_i)} ds \Big) \Big(\int_{t_{i-1}}^{t_i} \tau(t_i) e^{2\alpha t_{i-1}} \|\mathbf{u}_s(s)\|_2^2 ds \Big) \\
& \leq e^{2\alpha \Delta t} \sum_{i=1}^{n} \Big(\frac{\Delta t}{\tau(t_i)} \Big) \Big(\int_{t_{i-1}}^{t_i} \sigma(s) \|\mathbf{u}_s(s)\|_2^2 ds \Big).
\end{aligned}$$

When $0 < t_i < 1$, we have $\tau(t_i) = t_i = i\Delta t$. Hence

$$\begin{aligned}
\sum_{i=1}^{n} \Big(\frac{\Delta t}{\tau(t_i)} \Big) \Big(\int_{t_{i-1}}^{t_i} \sigma(s) \|\mathbf{u}_s(s)\|_2^2 ds \Big) & \leq \sum_{i=1}^{n} \frac{1}{i} \Big(\int_{t_{i-1}}^{t_i} \sigma(s) \|\mathbf{u}_s(s)\|_2^2 ds \Big) \\
& \leq \int_0^{t_n} \sigma(s) \|\mathbf{u}_s(s)\|_2^2 ds.
\end{aligned}$$

When $t_i \geq 1$, we have $\tau(t_i) = 1$ and then

$$\sum_{i=1}^{n} \Big(\frac{\Delta t}{\tau(t_i)} \Big) \Big(\int_{t_{i-1}}^{t_i} \sigma(s) \|\mathbf{u}_s(s)\|_2^2 ds \Big) \leq \Delta t \sum_{i=1}^{n} \Big(\int_{t_{i-1}}^{t_i} \sigma(s) \|\mathbf{u}_s(s)\|_2^2 ds \Big)$$

$$\leq \Delta t \int_0^{t_n} \sigma(s)\|\mathbf{u}_s(s)\|_2^2 ds.$$

We modify (4.17) for both $k = 1, 2$, using the fact $t - t_{i-1} \leq \tau(t)$ for $t \in [t_{i-1}, t_i]$ as

$$\begin{aligned}
&\Delta t \sum_{i=1}^{n} e^{2\alpha t_i} R^i(P_h \mathbf{e}^i) \\
\leq&\Delta t \sum_{i=1}^{n} e^{2\alpha t_i} \frac{1}{\Delta t} \int_{t_{i-1}}^{t_i} (s - t_{i-1})\|\mathbf{u}_{ss}(s)\| ds \; \|P_h \mathbf{e}^i\| \\
\leq&\Delta t \sum_{i=1}^{n} e^{2\alpha t_i} \Big(\frac{1}{\Delta t} \int_{t_{i-1}}^{t_i} (s - t_{i-1})\|\mathbf{u}_{ss}(s)\| ds \Big)^2 + \frac{1}{4}\Delta t \sum_{i=1}^{n} e^{2\alpha t_i} \|\mathbf{e}^i\|^2 \\
\leq&\frac{1}{\Delta t} \sum_{i=1}^{n} e^{2\alpha t_i} \Big(\int_{t_{i-1}}^{t_i} (s - t_{i-1}) ds \Big) \Big(\int_{t_{i-1}}^{t_i} (s - t_{i-1})\|\mathbf{u}_{ss}(s)\|^2 ds \Big) \\
&+ \frac{1}{4}\Delta t \sum_{i=1}^{n} e^{2\alpha t_i} \|\mathbf{e}^i\|^2 \\
\leq&\Delta t \sum_{i=1}^{n} e^{2\alpha t_i} \int_{t_{i-1}}^{t_i} \tau(s)\|\mathbf{u}_{ss}(s)\|^2 ds + \frac{1}{4}\Delta t \sum_{i=1}^{n} e^{2\alpha t_i} \|\mathbf{e}^i\|^2 \\
\leq&C\Delta t \int_0^{t_n} e^{2\alpha s} \tau(s)\|\mathbf{u}_{ss}(s)\|^2 ds + \frac{1}{4}\Delta t \sum_{i=1}^{n} e^{2\alpha t_i} \|\mathbf{e}^i\|^2.
\end{aligned}$$

Similarly we modify (4.18) and obtain

$$\begin{aligned}
\Delta t \sum_{i=1}^{n} e^{2\alpha t_i} |E^i(P_h \mathbf{e}^i)| \leq& C\Delta t \int_0^{t_n} e^{2\alpha s} \tau(s)(\|\mathbf{u}(s)\|_2^2 + \|\mathbf{u}_s(s)\|_2^2) ds \\
&+ \frac{1}{4}\Delta t \sum_{i=1}^{n} e^{2\alpha t_i} \|\mathbf{e}^i\|^2.
\end{aligned}$$

We use these modified estimates in the proof of Theorem 4.1 to complete the velocity estimates. Now, based on these modified estimates we can easily obtain the pressure estimate, similar to Theorem 4.2 which completes the rest of the proof. □

Remark 4.2. Similar to the semidiscrete case, here also we can not extend the analysis for $k \geq 3$ to obtain a better convergence rate.

5. Numerical experiments

In this section, we present some numerical experiments in support of our theoretical findings. We first verify the order of convergence of the error estimates for the velocity and the pressure. For simplicity, we use examples with known solutions. We then verify the effect of the grad-div stabilization for the Oldroyd model of order one with varying parameters. We consider two benchmark problems, namely, the lid-driven cavity and the flow around a cylinder, to show the same. Finally, we perform a few numerical simulations to find the appropriate choice of grad-div stabilization parameter. In all the cases, computations are done in FreeFem++ [25].

5.1. Known analytic solutions

We consider the Oldroyd model of order one in the domain $\Omega = [0,1]\times[0,1]$ subject to the homogeneous Dirichlet boundary condition. We approximate the equation using the Mini-element $(\mathbf{P}_1 b, P_1)$ [4] and the Taylor-Hood element $(\mathbf{P}_2, P_1)$ [8] over a regular triangulation of Ω. The domain is partitioned into triangles with sizes $h = 2^i,\ i = 2, 3, \ldots, 6$. To verify the theoretical results, we consider the following example:

Example 5.1. For the experiment, we take the forcing term $f(x,t)$ such that the solution of the problem is,

$$\begin{aligned}
u_1(x,t) &= -e^t(\cos(2\pi x)\sin(2\pi y) - \sin(2\pi y)),\\
u_2(x,t) &= e^t(\sin(2\pi x)\cos(2\pi y) - \sin(2\pi x)),\\
p(x,t) &= 2\pi e^t(\cos(2\pi y) - \cos(2\pi x)).
\end{aligned}$$

The theoretical analysis provides that the rate of convergences of the velocity and the pressure in L^2-norm are $\mathcal{O}(h+\Delta t)$ in case of the stable equal order finite element pair $(\mathbf{P}_1 b, P_1)$ and $\mathcal{O}(h^2+\Delta t)$ in case of the Taylor-Hood element $(\mathbf{P}_2, P_1)$. For the numerical experiments, we solve the problem for various values of μ, $\mu = 1, 10^{-2}, 10^{-4}, 10^{-6}$ and 10^{-8}, for each value of h with fixed $\delta = 0.1$ and $\gamma = 0.1\mu$. We set the grad-div parameter $\rho = h^2$ and $\Delta t = \mathcal{O}(h)$ for the MINI element and $\rho = 0.25$ and $\Delta t = \mathcal{O}(h^2)$ for the Taylor-Hood element for optimal values (see, Remark 3.3). In Figures 1 and 2, we present the absolute velocity and the pressure errors in L^2-norm for different values of μ, for the MINI element and for the Taylor-Hood element, respectively. From these graphs, we observe that the order of convergence coincides with the theoretical findings in the previous section (see, Theorem 4.1).

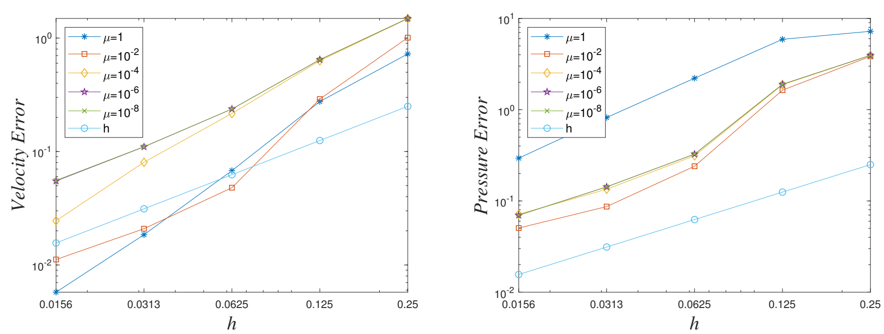

(a) Velocity (b) Pressure

Figure 1. Numerical errors in $\mathbf{L}^2$-norm for Example 5.1 with $\rho = h^2$ for $(\mathbf{P}_1 b, P_1)$ element.

5.2. Benchmark problem

We next look at a couple of benchmark problems.

Example 5.2. The first example is based on a benchmark problem related to the 2D lid-driven cavity flow on a unit square domain Ω with zero body forces, that is

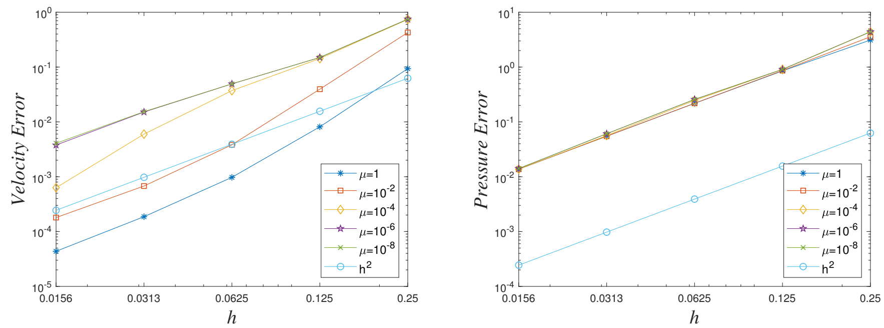

(a) Velocity (b) Pressure

Figure 2. Numerical errors in $\mathbf{L}^2$-norm for Example 5.1 with $\rho = 0.25$ for $(\mathbf{P}_2, P_1)$ element.

$\mathbf{f} = \mathbf{0}$ on Ω. We consider the no-slip boundary condition ($\mathbf{u} = (u_1, u_2)' = (0,0)'$) everywhere of the boundary except upper boundary and non-zero velocity ($\mathbf{u} = (u_1, u_2)' = (1,0)'$) on the upper boundary; see Figure 3.

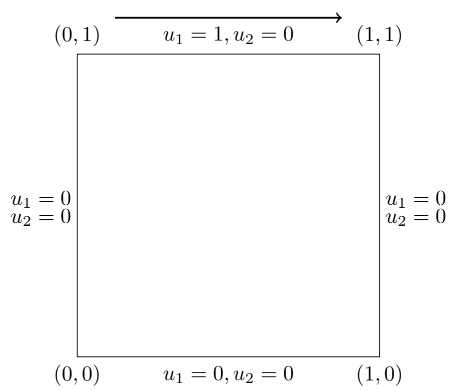

Figure 3. Lid-driven cavity flow.

For the numerical simulation, we approximate the velocity and pressure spaces by the lowest order stable Taylor-Hood element $(\mathbf{P}_2, P_1)$. The domain Ω is discretized over a regular triangulation with mesh size $h = 1/64$. We choose different values of parameter $\mu = 1, 10^{-2}, 10^{-4}$ with $\delta = 0.1$ and $\gamma = 0.1 \times \mu$ and fixed time step $\Delta t = 0.02$.

In Figures 4 and 5, we present the stream function, velocity vector, and pressure contour for the different values of μ and ρ (where ρ is the grad-div stabilization parameter). We consider both the cases with stabilization, that is, $\rho = 0.02$ and without stabilization, that is, $\rho = 0$. We plot the results at final time $T = 65$ for $\mu = 1, 10^{-2}$ and $T = 280$ for $\mu = 10^{-4}$. From these figures, we observe that we do not need stabilization for $\mu = 1$ and $\mu = 10^{-2}$. However, for $\mu = 10^{-4}$, the effect of stabilization can be seen; with stabilization, we get a stable steady-state solution, unlike the case with no stabilization. To emphasize this, we present the velocity profiles at one point on the cavity (in our case, we take (2/16,13/16)) for each time level in Figure 6. These observations indicate that for $\mu = 1$ and 10^{-2}, we get a steady state solution after a few time levels with or without stabilization. But for $\mu = 10^{-4}$, we find a periodic solution without any stabilization and a steady solution only with stabilization.

Example 5.3. We present another well-known benchmark problem related to the $2D$ flow around a cylinder with zero body forces ($\mathbf{f} = \mathbf{0}$) [31], to demonstrate the effectiveness of our scheme. The domain Ω is a channel of size $[0, 2.2] \times [0, 0.41]$ with a circle of diameter 0.1 located at $(0.2, 0.2)$ as shown in Figure 7. We denoted the boundaries of the domain Ω as: inflow boundary $\Gamma_{in} := \{x = 0\}$, outflow boundary $\Gamma_{out} := \{x = 2.2\}$, the remaining two wall $\Gamma_{wall} := \{y = 0, y = 0.41\}$ and the boundary of the circle $\Gamma_{cyl} := \{(x - 0.2)^2 + (y - 0.2)^2 = 0.0025\}$. The no-slip boundary, that is, $\mathbf{u} = (u_1, u_2) = (0, 0)$ has been considered at Γ_{wall} and Γ_{cyl} and the non-zero boundary, that is, $\mathbf{u}(0, y) = \mathbf{u}(2.2, y) = (u_d, 0)^{'}$, where

$$u_d = \frac{6}{0.14^2} \sin(\frac{\pi t}{8})(y(0.41 - y)), \quad 0 \leq y \leq 0.41$$

has been taken in the inflow and outflow boundaries Γ_{in} and Γ_{out} as shown in Figure 7.

For the test, we consider the motion of the fluid with $\mu = 10^{-3}, \delta = 0.1, \gamma = 0.1 * \mu$ occurring in the cylinder. The domain Ω is discretized over a regular triangulation with size $h = 1/64$. In this case also, we use Taylor-Hood element $(\mathbf{P}_2, P_1)$ to approximate the velocity and the pressure spaces and choose the grad div parameter $\rho = 0.25$. We take time step $\Delta t = 10^{-3}$ and the final time $T = 8$.

From the literature of the $2D$ flow around a cylinder for the well-known Navier-Stokes equations [31], we observe that a vortex sheet develops at the cylinder's bottom at around time $T = 4$. In fact, in our case also, we observe this phenomenon, see Figures 8 and 9. In these figures, we present the velocity field and stream function for different times $T = 5, 6, 7$ and 8 and observe that the vortices separated from the cylinder between the time $T = 5$ and $T = 6$, and the vortices are still visible at time $T = 8$. Further, we also calculate the drag coefficient $(c_d(t))$ and the lift coefficient $(c_l(t))$ at the cylinder as well as the differences in the pressure $(\Delta p(t))$ between the front and the back of the cylinder using the formula given in [31]. Finally, we plot the evolution of $c_d(t)$, $c_l(t)$, and $\Delta p(t)$ with respect to time in Figure 10. We compare the results of Oldroyd model of order one with Navier-Stokes equations and observe that both the results are coincide. Since, in this case we consider $\gamma = 10^{-4}$ and we know that as $\gamma \to 0$ the solution of Oldroyd model of order one behave like the solution of Navier-Stokes equations. In addition, we mark the maximum value of $c_d(t)$, $c_l(t)$, and the final value of $\Delta p(t)$ in the Figure 10.

5.3. Choice of grad-div parameter

As discussed in the introduction, the choice of grad-div stabilization parameter plays a vital role in numerical simulations. Here we present a few numerical examples to find a suitable choice of grad-div parameter for the Oldroyd model of order one.

We use the known solution of Example 5.1 for our current experiment. The numerical simulations are performed for different values of ρ that lie between 10^{-3} to 10^4, approximating the equation using the MINI element $(\mathbf{P}_1 b, P_1)$ and the Taylor-Hood element $(\mathbf{P}_2, P_1)$. The numerical results are computed for three successively finer meshes, with mesh sizes $h = 1/8, 1/16$ and $1/32$, for both union jack (criss-cross) and Delaunay type triangulation, and for $\mu = 1, 10^{-2}, 10^{-4}, 10^{-6}$ and 10^{-8}.

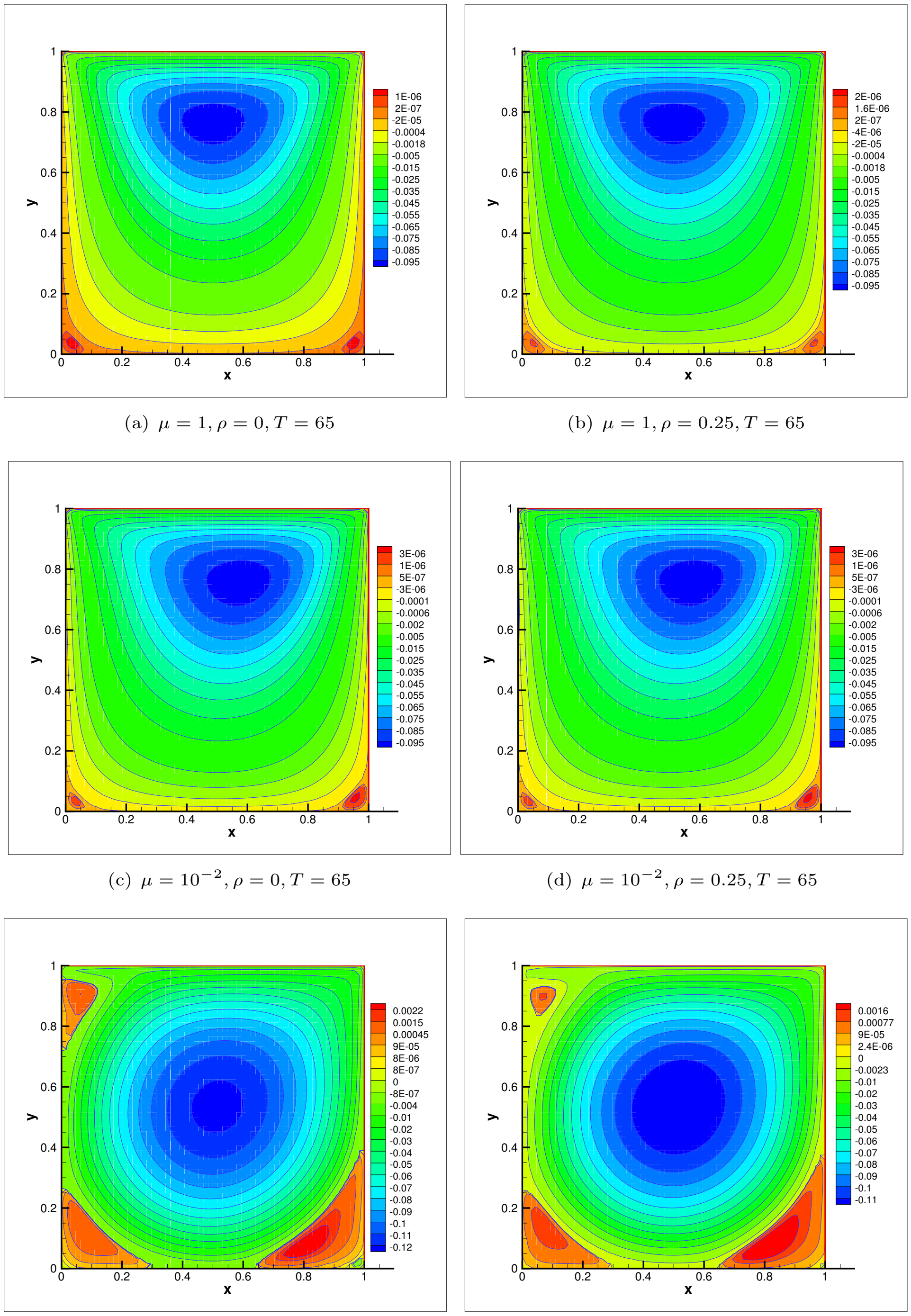

(a) $\mu = 1, \rho = 0, T = 65$

(b) $\mu = 1, \rho = 0.25, T = 65$

(c) $\mu = 10^{-2}, \rho = 0, T = 65$

(d) $\mu = 10^{-2}, \rho = 0.25, T = 65$

(e) $\mu = 10^{-4}, \rho = 0, T = 280$

(f) $\mu = 10^{-4}, \rho = 0.25, T = 280$

Figure 4. Stream function for Example 5.2 for $h = 1/64$.

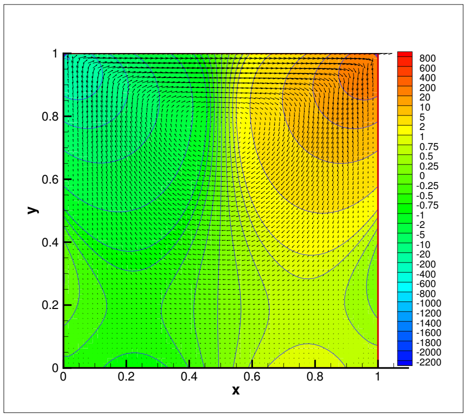

(a) $\mu = 1, \rho = 0, T = 65$

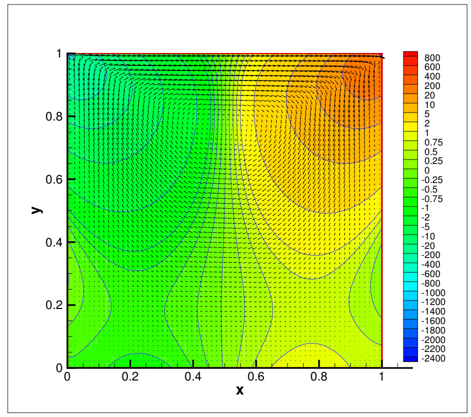

(b) $\mu = 1, \rho = 0.25, T = 65$

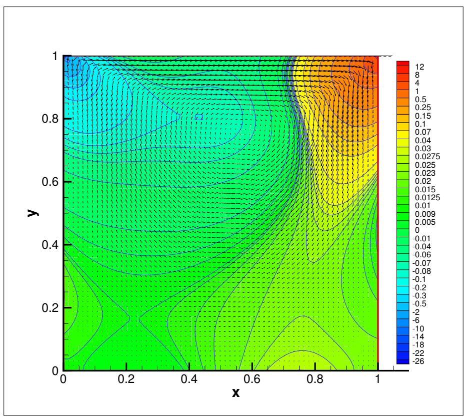

(c) $\mu = 10^{-2}, \rho = 0, T = 65$

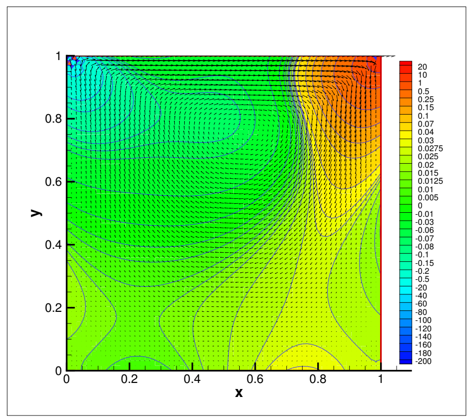

(d) $\mu = 10^{-2}, \rho = 0.25, T = 65$

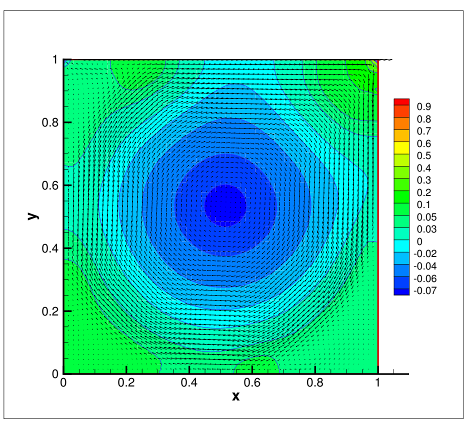

(e) $\mu = 10^{-4}, \rho = 0, T = 280$

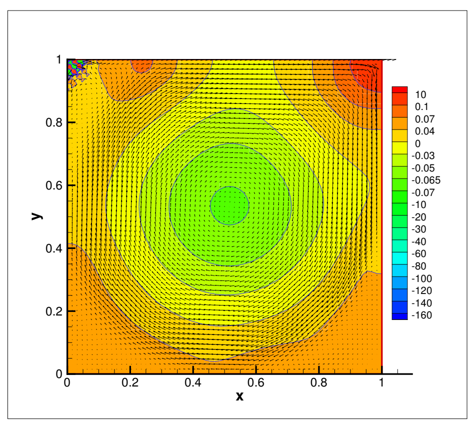

(f) $\mu = 10^{-4}, \rho = 0.25, T = 280$

Figure 5. Velocity vector and pressure contour for Example 5.2 for $h = 1/64$.

Figures 11 and 12 represent the velocity and the pressure errors graphs with respect

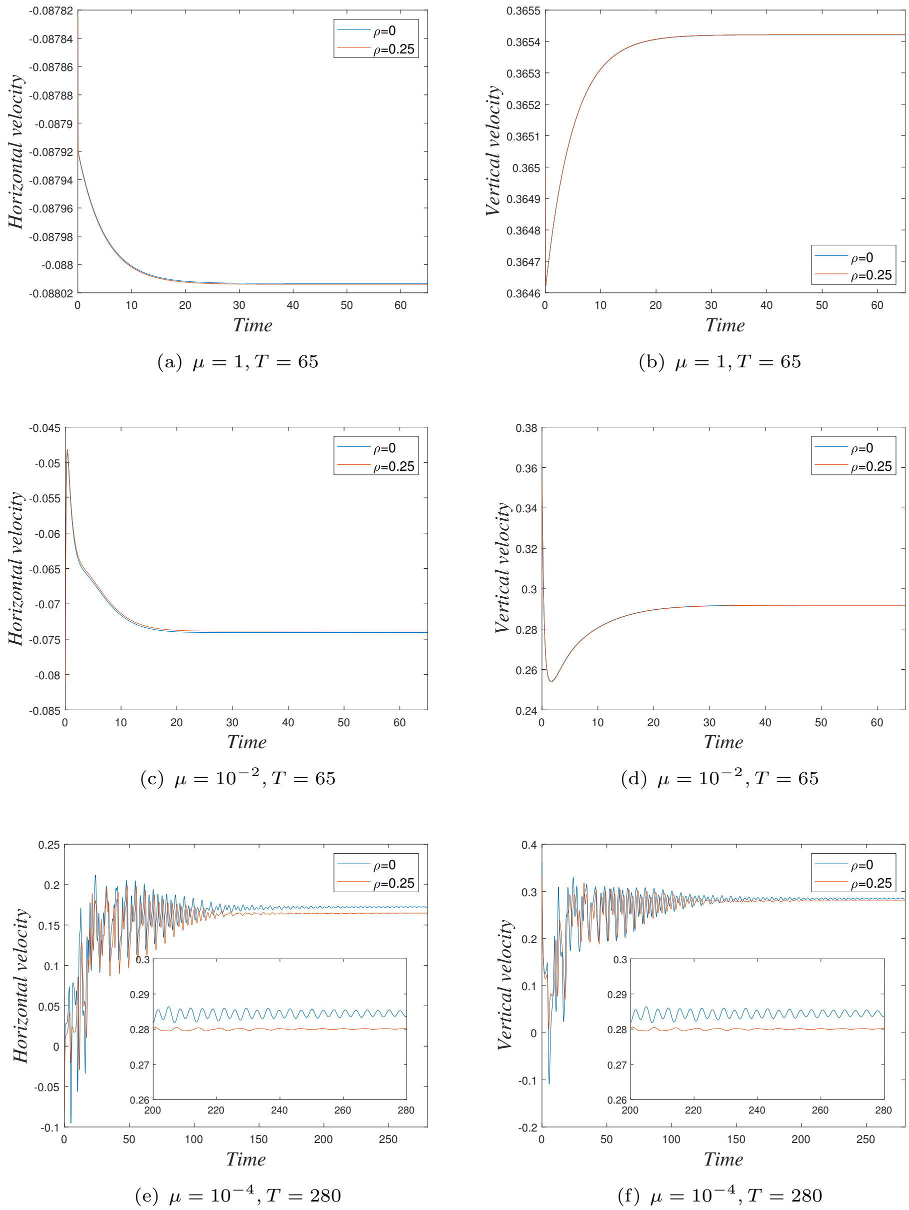

(a) $\mu = 1, T = 65$ (b) $\mu = 1, T = 65$

(c) $\mu = 10^{-2}, T = 65$ (d) $\mu = 10^{-2}, T = 65$

(e) $\mu = 10^{-4}, T = 280$ (f) $\mu = 10^{-4}, T = 280$

Figure 6. Velocity profile at monitoring point (2/16,13/16) for Example 5.2 for $h = 1/64$.

to the grad-div stabilization parameter ρ for the MINI element and the Taylor-Hood element, respectively. For each value of μ, we mark these error graphs for minimum error, depicting the value of ρ. Overall these figures give us a rough picture of how the grad-div parameter ρ changes with h and μ. We observe that for $\mathbf{L}^2$ error of velocity, a suitable range of ρ would be from 10^{-1} to 10^1. However, for $\mathbf{H}^1$ error of velocity and for L^2 error of pressure, a suitable range of ρ is 10^{-1} to 10^4.

We also present the values of grad-div parameter ρ, that minimize the $\mathbf{L}^2$ and

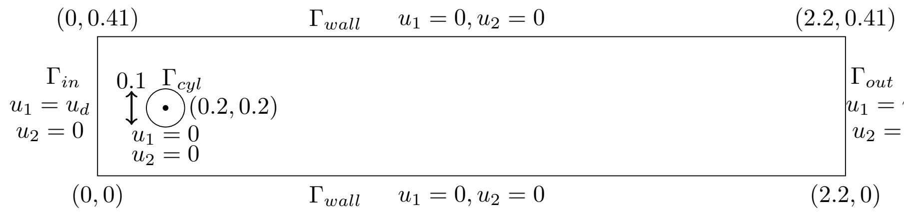

Figure 7. Domain Ω for flow past cylinder.

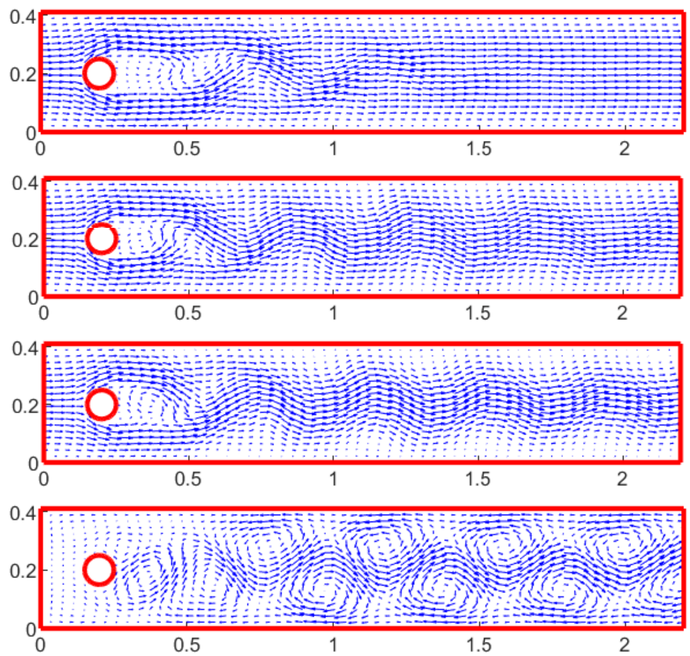

Figure 8. Velocity field for Example 5.3 for $T = 5, 6, 7, 8$.

$\mathbf{H}^1$ errors for the velocity and L^2 error for the pressure. In Tables 1-4, we present the corresponding minimum errors and the errors for the standard choice of grad-div parameter $\rho = 1$ for different values of h. We have used boldface for the minimizing value of ρ in each case. We also observe that we do not get any stable solution for $\mu = 10^{-6}$ and $\mu = 10^{-8}$ when we use Taylor-Hood element to approximate the equation over Delaunay triangulation with mesh size $h = 1/8$ or $h = 1/16$. However, for $\mu = 10^{-6}$ if we take $h = 1/32$, we get a stable solution.

6. Conclusion

We have considered here, an inf-sup mixed finite element method for the Oldroyd model of order one with grad-div stabilization. We have obtained the error estimates

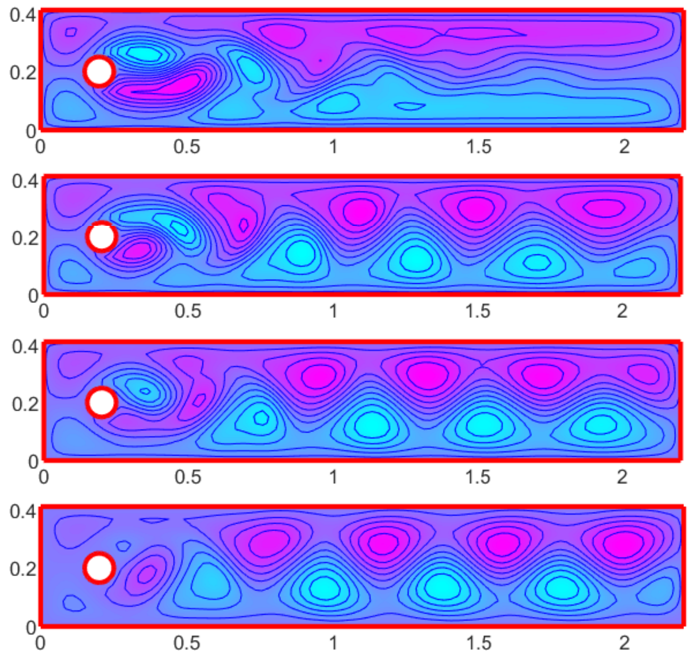

Figure 9. Stream function for Example 5.3 for $T = 5, 6, 7, 8$.

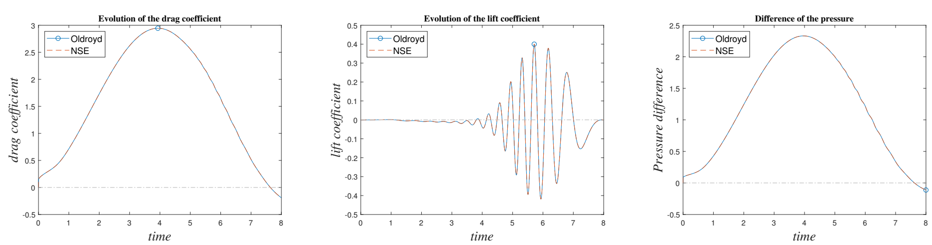

Figure 10. Drag coefficient, lift coefficient, and pressure difference for Example 5.3.

in $L^\infty(\mathbf{L}^2)$-norm for the velocity and $L^2(\mathbf{L}^2)$-norm for the pressure in the semidiscrete case as well as in the fully discrete case with the error bounds independent of the inverse power of μ. We have carried out our analysis for both $\mathbf{H}^m$-smooth and $\mathbf{H}^2$-smooth initial data. Finally, we have briefly looked at suitable values of the grad-div parameter for the Oldroyd model of order one.

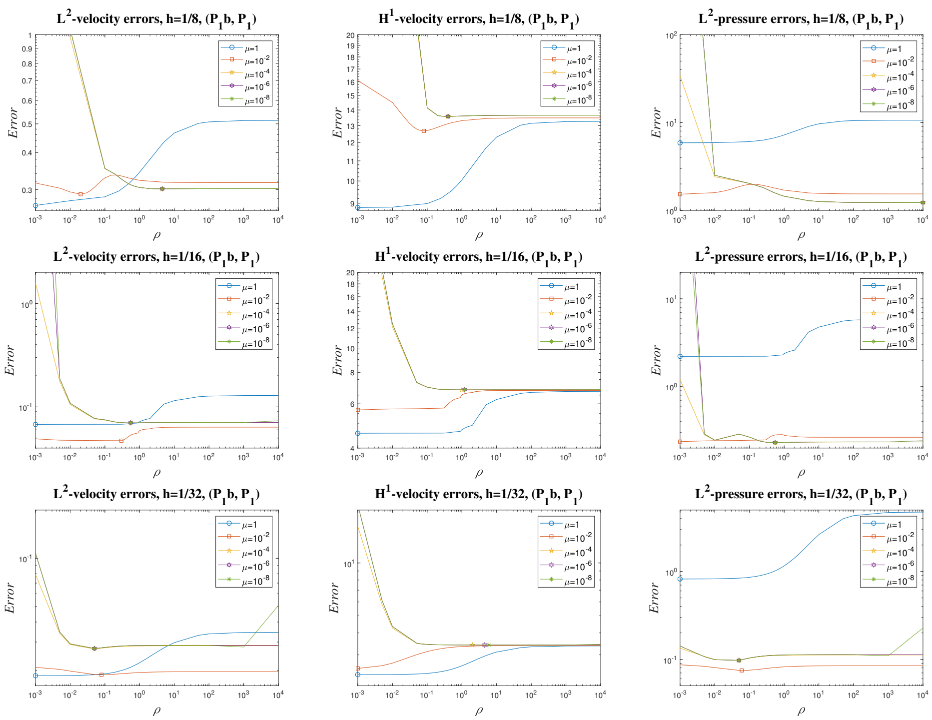

Figure 11. Velocity and pressure errors vs stabilization parameter for $(\mathbf{P}_1 b, P_1)$ element on union jack triangulation.

Table 1. Minimum errors and corresponding stabilization parameter ρ for $(\mathbf{P}_1 b, P_1)$ element on union jack triangulation.

	Velocity errors in L^2-norm			Velocity errors in H^1-norm			Pressure errors in L^2-norm		
μ	ρ	Min	Std.(ρ=1)	ρ	Min	Std.(ρ=1)	ρ	Min	Std.(ρ=1)
h=1/8									
1	**0.001**	0.27419	0.34335	**0.001**	8.81884	10.05271	**0.001**	5.8799	7.21910
1e-2	**0.02**	0.28931	0.32214	**0.08**	12.6806	13.31144	**0.001**	1.5288	1.70077
1e-4	**4.5**	0.30166	0.30490	**0.4**	13.5764	13.60262	**10000**	1.23236	1.45157
1e-6	**4.5**	0.30166	0.30486	**0.4**	13.5823	13.60660	**10000**	1.22929	1.44892
1e-8	**4.5**	0.30166	0.30486	**0.4**	13.5823	13.60664	**10000**	1.22746	1.44890
h=1/16									
1	**0.001**	0.06776	0.08406	**0.001**	4.58129	5.16855	**0.001**	2.21019	2.91551
1e-2	**0.01**	0.04718	0.06249	**0.001**	5.67357	6.71433	**0.001**	0.23700	0.26881
1e-4	**0.55**	0.07000	0.07011	**1.0**	6.82155	6.82155	**0.55**	0.23076	0.23147
1e-6	**0.55**	0.07017	0.07030	**1.2**	6.82284	6.82290	**0.55**	0.23090	0.23174
1e-8	**0.55**	0.07015	0.07030	**1.2**	6.82285	6.82291	**0.55**	0.23090	0.23175
h=1/32									
1	**0.001**	0.01848	0.02229	**0.001**	2.31312	2.59893	**0.001**	0.82050	1.15744
1e-2	**0.08**	0.01875	0.01936	**0.001**	2.51021	3.34415	**0.06**	0.07475	0.08212
1e-4	**0.05**	0.02717	0.02836	**2.0**	3.41308	3.41329	**0.05**	0.09716	0.11123
1e-6	**0.05**	0.02735	0.02855	**4.5**	3.41332	3.41436	**0.05**	0.09740	0.11218
1e-8	**0.05**	0.02735	0.02855	**6.0**	3.41334	3.41437	**0.05**	0.09740	0.11217

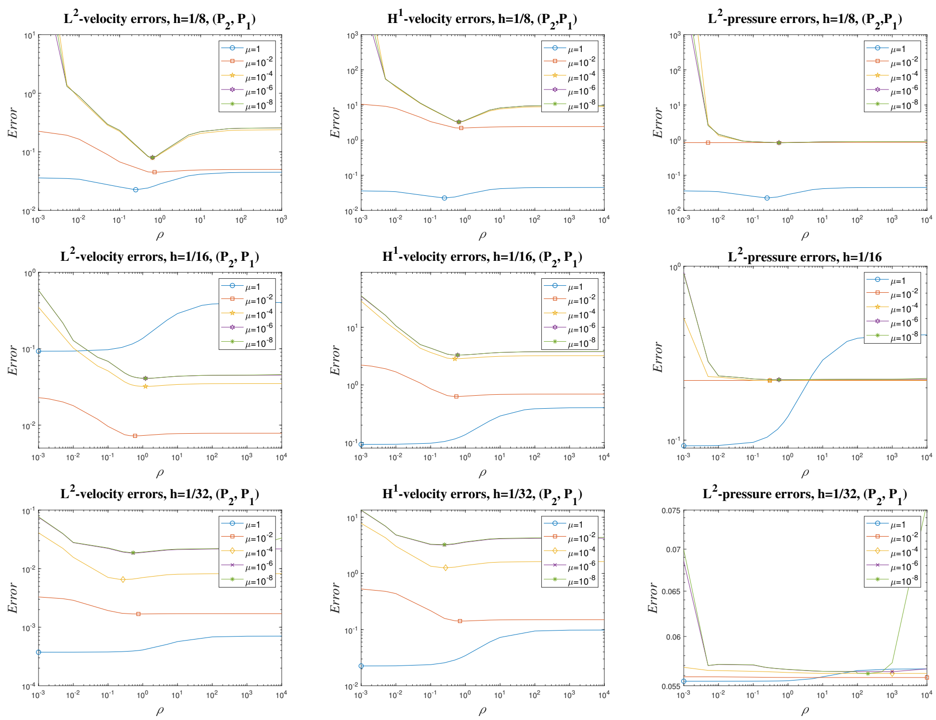

Figure 12. Velocity and pressure errors vs stabilization parameter for $(\mathbf{P}_2, P_1)$ element on union jack triangulation.

Table 2. Minimum errors and corresponding stabilization parameter ρ for $(\mathbf{P}_2, P_1)$ element on union jack triangulation.

	Velocity errors in L^2-norm			Velocity errors in H^1-norm			Pressure errors in L^2-norm		
μ	ρ	Min	Std.(ρ=1)	ρ	Min	Std.(ρ=1)	ρ	Min	Std.(ρ=1)
h=1/8									
1	**0.001**	0.01011	0.01365	**0.001**	0.40921	0.54307	**0.001**	0.86810	0.88401
1e-2	**0.73**	0.04502	0.04525	**0.76**	2.21141	2.21968	**0.005**	0.84583	0.85761
1e-4	**0.65**	0.07898	0.09129	**0.65**	3.26339	3.57391	**0.55**	0.84359	0.84799
1e-6	**0.65**	0.08016	0.09427	**0.65**	3.29902	3.66404	**0.55**	0.84148	0.84708
1e-8	**0.65**	0.08017	0.09430	**0.65**	3.29939	3.66500	**0.55**	0.84146	0.84707
h=1/16									
1	**0.001**	0.00133	0.00182	**0.001**	0.09276	0.13683	**0.001**	0.22091	0.22190
1e-2	**0.6**	0.00723	0.00731	**0.55**	0.63038	0.63938	**0.3**	0.22028	0.22029
1e-4	**1.2**	0.03211	0.03214	**0.5**	2.84648	2.89919	**0.3**	0.22017	0.22060
1e-6	**1.2**	0.04087	0.04098	**0.6**	3.29495	3.32761	**0.55**	0.22258	0.22268
1e-8	**1.2**	0.04099	0.04110	**0.6**	3.30041	3.33304	**0.55**	0.22262	0.22271
h=1/32									
1	**0.001**	0.00037	0.00041	**0.001**	0.02253	0.03440	**0.001**	0.05545	0.05549
1e-2	**0.73**	0.00168	0.00168	**0.7**	0.14200	0.14244	**10000**	0.05581	0.05581
1e-4	**0.27**	0.00652	0.00704	**0.27**	1.26200	1.38753	**1000**	0.05621	0.05630
1e-6	**0.55**	0.01876	0.01888	**0.25**	3.26332	3.59116	**1000**	0.05638	0.05660
1e-8	**0.55**	0.01876	0.01924	**0.25**	3.30041	3.65619	**200**	0.05619	0.05662

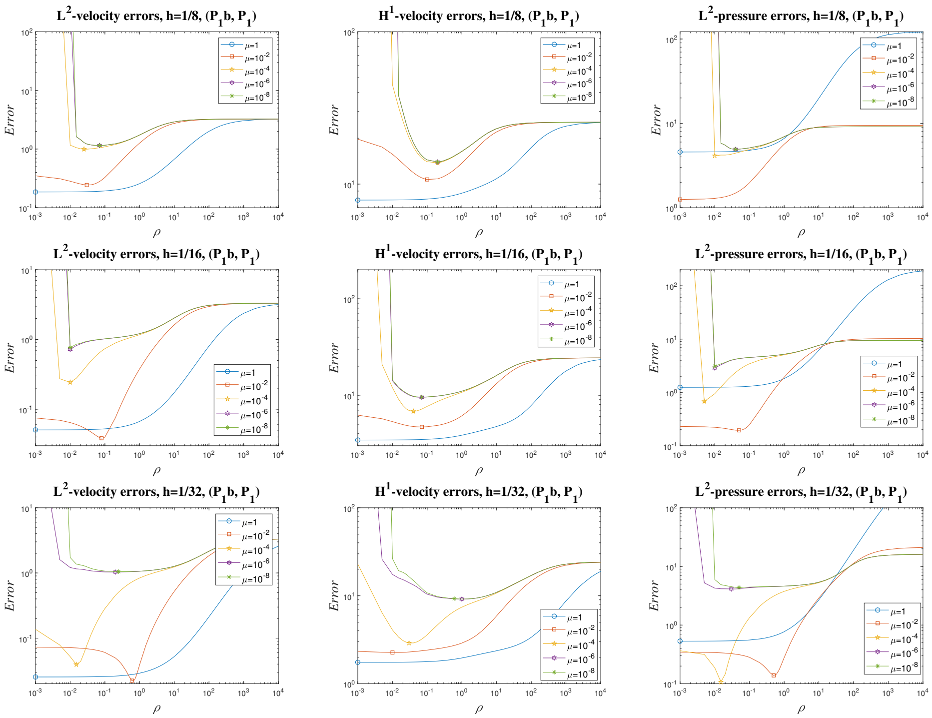

Figure 13. Velocity and pressure errors vs stabilization parameter for $(\mathbf{P}_1 b, P_1)$ element on Delaunay type triangulation.

Table 3. Minimum errors and corresponding stabilization parameter ρ for $(\mathbf{P}_1 b, P_1)$ element Delaunay type triangulation.

	Velocity errors in L^2-norm			Velocity errors in H^1-norm			Pressure errors in L^2-norm		
μ	ρ	Min	Std.(ρ=1)	ρ	Min	Std.(ρ=1)	ρ	Min	Std.(ρ=1)
h=1/8									
1	**0.001**	0.185122	0.25705	**0.001**	7.85131	8.71753	**0.001**	4.57057	6.63177
1e-2	**0.03**	0.24378	1.26223	**0.1**	10.7217	13.73449	**0.001**	1.25154	5.65359
1e-4	**0.025**	0.99323	1.73066	**0.2**	13.7813	16.35411	**0.01**	4.13082	6.93560
1e-6	**0.07**	1.15039	1.73890	**0.2**	13.9664	16.40470	**0.04**	4.91701	6.95563
1e-8	**0.07**	1.15148	1.73898	**0.2**	13.9684	16.40520	**0.04**	4.92269	6.95584
h=1/16									
1	**0.001**	0.05050	0.06689	**0.001**	3.43433	3.85367	**0.001**	1.24350	1.81684
1e-2	**0.08**	0.03853	0.24232	**0.07**	4.69254	6.12371	**0.05**	0.19402	1.92537
1e-4	**0.01**	0.24278	1.17155	**0.04**	6.80301	10.73557	**0.005**	0.67628	5.06504
1e-6	**0.01**	0.72179	1.21321	**0.07**	9.52722	11.02760	**0.01**	2.86844	5.20610
1e-8	**0.01**	0.76774	1.21371	**0.07**	9.57175	11.02760	**0.01**	3.10471	5.20615
h=1/32									
1	**0.001**	0.02538	0.02904	**0.001**	1.75240	1.96327	**0.001**	0.53194	0.77064
1e-2	**0.6**	0.02231	0.03898	**0.01**	2.26439	2.89959	**0.5**	0.13858	0.27880
1e-4	**0.015**	0.03936	0.83711	**0.03**	2.90569	7.41920	**0.015**	0.10728	3.75283
1e-6	**0.2**	1.03245	1.06105	**1.0**	9.15781	9.15781	**0.03**	4.12698	4.60846
1e-8	**0.25**	1.04678	1.06412	**1.0**	9.18281	9.18281	**0.05**	4.37574	4.61964

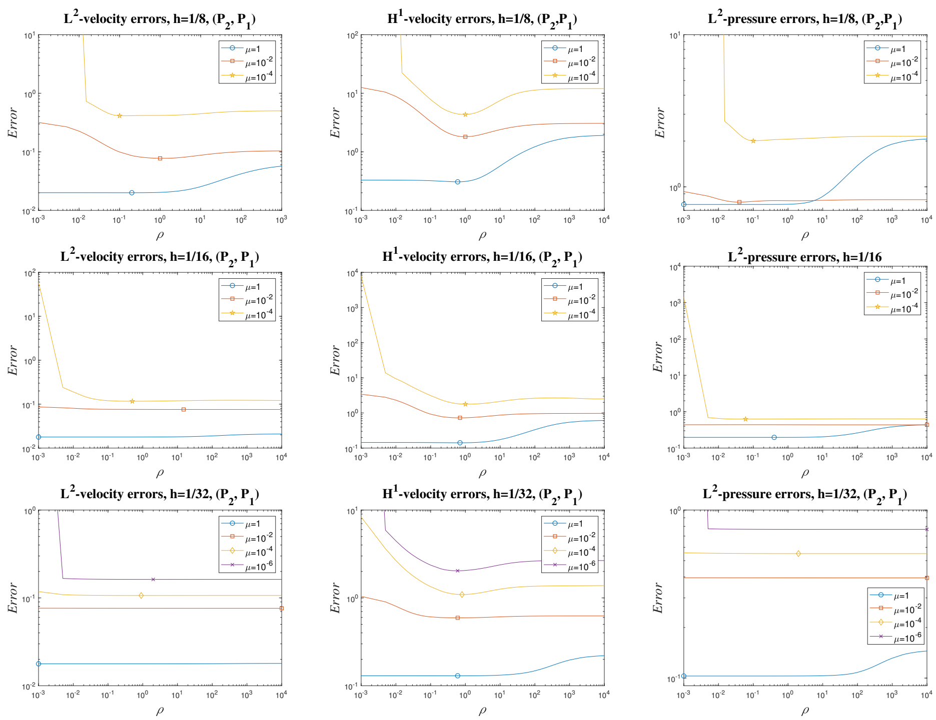

Figure 14. Velocity and pressure errors vs stabilization parameter for $(\mathbf{P}_2, P_1)$ element on Delaunay type triangulation.

Table 4. Minimum errors and corresponding stabilization parameter ρ for $(\mathbf{P}_2, P_1)$ element on Delaunay type triangulation ('-' represent no convergence).

	Velocity errors in L^2-norm			Velocity errors in H^1-norm			Pressure errors in L^2-norm		
μ	ρ	Min	Std.(ρ=1)	ρ	Min	Std.(ρ=1)	ρ	Min	Std.(ρ=1)
h=1/8									
1	**0.2**	0.02001	0.02031	**0.6**	0.30745	0.31173	**0.001**	0.76559	0.76824
1e-2	**1.0**	0.07746	0.07746	**1.0**	1.80654	1.80654	**0.04**	0.79381	0.81041
1e-4	**0.1**	0.41249	0.41825	**1.0**	4.32884	4.32884	**0.1**	2.00494	2.05792
1e-6	**-**	-	-	**-**	-	-	**-**	-	-
1e-8	**-**	-	-	**-**	-	-	**-**	-	-
h=1/16									
1	**0.001**	0.01785	0.01786	**0.7**	0.14177	0.14204	**0.4**	0.19729	0.19737
1e-2	**15**	0.07571	0.07592	**0.7**	0.72667	0.72999	**10000**	0.43669	0.43944
1e-4	**0.5**	0.11650	0.11678	**1.0**	1.77762	1.7762	**0.06**	0.62709	0.63073
1e-6	**-**	-	-	**-**	-	-	**-**	-	-
1e-8	**-**	-	-	**-**	-	-	**-**	-	-
h=1/32									
1	**0.001**	0.01777	0.01777	**0.6**	0.12987	0.12989	**0.001**	0.10288	0.10290
1e-2	**10000**	0.07621	0.07625	**0.6**	0.59381	0.59427	**10000**	0.39478	0.39511
1e-4	**0.9**	0.10657	0.10658	**0.8**	1.09028	1.09397	**2.0**	0.55087	0.55088
1e-6	**2.0**	0.162439	0.16246	**0.6**	2.03721	2.05409	**10000**	0.76746	0.76753
1e-8	**-**	-	-	**-**	-	-	**-**	-	-

References

[1] M. Abbaszadeh and M. Dehghan, *Investigation of the Oldroyd model as a generalized incompressible Navier–Stokes equation via the interpolating stabilized element free Galerkin technique*, Applied Numerical Mathematics, 2020, 150, 274–294.

[2] R. Adams, *Sobolev Spaces*, Press, New York, 1975.

[3] N. Ahmed, *On the grad-div stabilization for the steady Oseen and Navier-Stokes equations*, Calcolo, 2017, 54, 471–501.

[4] D. N. Arnold, F. Brezzi and M. Fortin, *A stable finite element for the Stokes equations*, Calcolo, 1984, 21(4), 337–344.

[5] B. Bir and D. Goswami, *On a three step two-grid finite element method for the Oldroyd model of order one*, ZAMM-Journal of Applied Mathematics and Mechanics/Zeitschrift für Angewandte Mathematik und Mechanik, 2021, 101(11), e202000373.

[6] B. Bir, D. Goswami and A. K. Pani, *Backward Euler method for the equations of motion arising in Oldroyd model of order one with nonsmooth initial data*, IMA Journal of Numerical Analysis, 2022, 42(4), 3529–3570.

[7] B. Bir, D. Goswami and A. K. Pani, *Finite element penalty method for the Oldroyd model of order one with non-smooth initial data*, Computational Methods in Applied Mathematics, 2022, 22(2), 297–325.

[8] D. Boffi, F. Brezzi and M. Fortin, *Mixed Finite Element Methods and Applications*, 44, Springer, 2013.

[9] M. Braack and E. Burman, *Local projection stabilization for the Oseen problem and its interpretation as a variational multiscale method*, SIAM Journal on Numerical Analysis, 2006, 43(6), 2544–2566.

[10] S. C. Brenner, *The Mathematical Theory of Finite Element Methods*, Springer, 2008.

[11] F. Brezzi and A. Russo, *Choosing bubbles for advection-diffusion problems*, Mathematical Models and Methods in Applied Sciences, 1994, 4(04), 571–587.

[12] A. N. Brooks and T. J. Hughes, *Streamline upwind/Petrov-Galerkin formulations for convection dominated flows with particular emphasis on the incompressible Navier-Stokes equations*, Computer Methods in Applied Mechanics and Engineering, 1982, 32(1–3), 199–259.

[13] E. Burman and P. Hansbo, *Edge stabilization for Galerkin approximations of convection–diffusion–reaction problems*, Computer Methods in Applied Mechanics and Engineering, 2004, 193(15–16), 1437–1453.

[14] P. G. Ciarlet, *The Finite Element Method for Elliptic Problems*, SIAM, 2002.

[15] H. Dallmann, D. Arndt and G. Lube, *Local projection stabilization for the Oseen problem*, IMA Journal of Numerical Analysis, 2016, 36(2), 796–823.

[16] L. P. Franca and T. J. Hughes, *Two classes of mixed finite element methods*, Computer Methods in Applied Mechanics and Engineering, 1988, 69(1), 89–129.

[17] J. de Frutos, B. García-Archilla, V. John and J. Novo, *Grad-div stabilization for the evolutionary Oseen problem with inf-sup stable finite elements*, Journal of Scientific Computing, 2016, 66(3), 991–1024.

[18] J. de Frutos, B. García-Archilla, V. John and J. Novo, *Analysis of the grad-div stabilization for the time-dependent Navier–Stokes equations with inf-sup stable finite elements*, Advances in Computational Mathematics, 2018, 44, 195–225.

[19] K. J. Galvin, A. Linke, L. G. Rebholz and N. E. Wilson, *Stabilizing poor mass conservation in incompressible flow problems with large irrotational forcing and application to thermal convection*, Computer Methods in Applied Mechanics and Engineering, 2012, 237, 166–176.

[20] D. Goswami, P. D. Damázio, J. Y. Yuan and B. Bir, *Two-grid finite element Galerkin approximation of equations of motion arising in Oldroyd fluids of order one with non-smooth initial data*, Computational Mathematics and Mathematical Physics, 2023, 63(4), 659–686.

[21] D. Goswami and A. K. Pani, *A priori error estimates for semidiscrete finite element approximations to the equations of motion arising in Oldroyd fluids of order one*, International Journal of Numerical Analysis & Modeling, 2011, 8(2).

[22] Y. Guo and Y. He, *Crank–Nicolson extrapolation and finite element method for the Oldroyd fluid with the midpoint rule*, Journal of Computational and Applied Mathematics, 2022, 415, 114453.

[23] W.-W. Han, Y.-L. Jiang and Z. Miao, *Numerical analysis of projection methods for the time-dependent Navier-Stokes equations with modular grad-div stabilization*, Computers & Mathematics with Applications, 2023, 141, 145–158.

[24] Y. He, Y. Lin, S. S. Shen, et al., *Finite element approximation for the viscoelastic fluid motion problem*, Journal of Computational and Applied Mathematics, 2003, 155(2), 201–222.

[25] F. Hecht, *New development in FreeFem++*, Journal of Numerical Mathematics, 2012, 20(3–4), 251–266.

[26] J. G. Heywood and R. Rannacher, *Finite element approximation of the nonstationary Navier–Stokes problem. I. Regularity of solutions and second-order error estimates for spatial discretization*, SIAM Journal on Numerical Analysis, 1982, 19(2), 275–311.

[27] J. G. Heywood and R. Rannacher, *Finite-element approximation of the nonstationary Navier–Stokes problem, Part IV: Error analysis for second-order time discretization*, SIAM Journal on Numerical Analysis, 1990, 27(2), 353–384.

[28] A. T. Hill and E. Süli, *Approximation of the global attractor for the incompressible Navier–Stokes equations*, IMA Journal of Numerical Analysis, 2000, 20(4), 633–667.

[29] E. W. Jenkins, V. John, A. Linke and L. G. Rebholz, *On the parameter choice in grad-div stabilization for the Stokes equations*, Advances in Computational Mathematics, 2014, 40, 491–516.

[30] Y. Jiang, B. Zheng and Y. Shang, *A parallel grad-div stabilized finite element algorithm for the Stokes equations with damping*, Computers & Mathematics with Applications, 2023, 135, 171–192.

[31] V. John, *Reference values for drag and lift of a two-dimensional time-dependent flow around a cylinder*, International Journal for Numerical Methods in Fluids, 2004, 44(7), 777–788.

[32] V. John and A. Kindl, *Numerical studies of finite element variational multiscale methods for turbulent flow simulations*, Computer Methods in Applied Mechanics and Engineering, 2010, 199(13–16), 841–852.

[33] C. Liu and Z. Si, *An incremental pressure correction finite element method for the time-dependent Oldroyd flows*, Applied Mathematics and Computation, 2019, 351, 99–115.

[34] G. Matthies, N. I. Ionkin, G. Lube and L. Röhe, *Some remarks on residual-based stabilisation of inf-sup stable discretisations of the generalised Oseen problem*, Computational Methods in Applied Mathematics, 2009, 9(4), 368–390.

[35] M. T. Mohan, *Deterministic and stochastic equations of motion arising in Oldroyd fluids of order one: Existence, uniqueness, exponential stability and invariant measures*, Stochastic Analysis and Applications, 2020, 38(1), 1–61.

[36] J. Oldroyd, *Non-Newtonian flow of liquids and solids*, in *Rheology*, Elsevier, 1956, 653–682.

[37] M. A. Olshanskii, *A low order Galerkin finite element method for the Navier–Stokes equations of steady incompressible flow: A stabilization issue and iterative methods*, Computer Methods in Applied Mechanics and Engineering, 2002, 191(47–48), 5515–5536.

[38] M. A. Olshanskii, G. Lube, T. Heister and J. Löwe, *Grad–div stabilization and subgrid pressure models for the incompressible Navier–Stokes equations*, Computer Methods in Applied Mechanics and Engineering, 2009, 198(49–52), 3975–3988.

[39] M. A. Olshanskii and A. Reusken, *Grad-div stabilization for Stokes equations*, Mathematics of Computation, 2004, 73(248), 1699–1718.

[40] A. K. Pani and J. Y. Yuan, *Semidiscrete finite element Galerkin approximations to the equations of motion arising in the Oldroyd model*, IMA Journal of Numerical Analysis, 2005, 25(4), 750–782.

[41] A. K. Pani, J. Y. Yuan and P. D. Damázio, *On a linearized backward Euler method for the equations of motion of Oldroyd fluids of order one*, SIAM Journal on Numerical Analysis, 2006, 44(2), 804–825.

[42] L. Röhe and G. Lube, *Analysis of a variational multiscale method for Large–Eddy simulation and its application to homogeneous isotropic turbulence*, Computer Methods in Applied Mechanics and Engineering, 2010, 199(37–40), 2331–2342.

[43] Y. Shang, *A two-level finite element method with grad-div stabilizations for the incompressible Navier–Stokes equations*, Journal of Computational and Applied Mathematics, 2024, 446(17), 115865.

[44] Y. Shang, J. Zhu and B. Zheng, *A parallel finite element discretization algorithm based on grad-div stabilization for the Navier–Stokes equationss*, Journal of Mathematical Fluid Mechanics, 2024, 26(3), 42.

[45] K. Wang, Y. He and X. Feng, *On error estimates of the penalty method for the viscoelastic flow problem I: Time discretization*, Applied Mathematical Modelling, 2010, 34(12), 4089–4105.

[46] K. Wang, Y. He and X. Feng, *On error estimates of the fully discrete penalty method for the viscoelastic flow problem*, International Journal of Computer Mathematics, 2011, 88(10), 2199–2220.

[47] K. Wang, Y. He and Y. Shang, *Fully discrete finite element method for the viscoelastic fluid motion equations*, Discrete & Continuous Dynamical Systems-B, 2010, 13(3), 665.

[48] J. Wen, Z. Chen and Y. He, *The analogue of grad-div stabilization in DG method for a coupled Stokes and Darcy problem*, Computers & Mathematics with Applications, 2023, 149(3), 99–114.

[49] Y. Yang, Y. Lei and Z. Si, *Unconditional stability and error estimates of the modified characteristics fem for the time-dependent viscoelastic Oldroyd flows*, Advances in Applied Mathematics and Mechanics, 2020, 13(2), 311–332.

[50] T. Zhang and Y. Qian, *Stability analysis of several first order schemes for the Oldroyd model with smooth and nonsmooth initial data*, Numerical Methods for Partial Differential Equations, 2018, 34(6), 2180–2216.

[51] T. Zhang, Y. Qian, T. Jiang and J. Yuan, *Stability and convergence of the higher projection method for the time-dependent viscoelastic flow problem*, Journal of Computational and Applied Mathematics, 2018, 338, 1–21.